11142 *Inorg. Chem.* **2010**, *49*, 11142–11157
DOI: 10.1021/ic101741e

Inorganic Chemistry
Article

Vibrational Spectra, Crystal Structures, Constitutional and Rotational Isomerism of FC(O)SCN and FC(O)NCS

Luis A. Ramos,[†] Sonia E. Ulic,[†,‡] Rosana M. Romano,[†] Mauricio F. Erben,[†] Christian W. Lehmann,[§] Eduard Bernhardt,[⊥] Helmut Beckers,[⊥] Helge Willner,[⊥] and Carlos O. Della Védova*[,†,¶]

[†]*CEQUINOR (UNLP-CONICET), Departamento de Química, Facultad de Ciencias Exactas, Universidad Nacional de La Plata, 47 esq. 115, 1900 La Plata, República Argentina,* [‡]*Departamento de Ciencias Básicas, Universidad Nacional de Luján, Rutas 5 y 7, 6700 Luján, Argentina,* [§]*Max-Planck-Institut für Kohlenforschung, D-45470 Mülheim/Ruhr, Germany,* [⊥]*Fachbereich C, Anorganische Chemie, Bergische Universität Wuppertal, 42097 Wuppertal, Germany, and* [¶]*Laboratorio de Servicios a la Industria y al Sistema Científico (UNLP-CIC-CONICET), Buenos Aires, República Argentina*

Received August 26, 2010

Fluorocarbonyl thio- and isothiocyanate, FC(O)SCN and FC(O)NCS, were fully characterized by IR (gas, Ar and N_2 matrixes), Raman (liquid and solid), UV (gas), and ^{13}C NMR (liquid) spectroscopy, as well as single-crystal X-ray diffraction. Their vibrational and conformational properties were analyzed using matrix isolation techniques guided by quantum chemical calculation at the ab initio [MP2 and CCSD(T)], density functional theory B3LYP, and CBS-QB3 levels of theory. A complete assignment of the fundamental modes of FC(O)SCN was performed. In both the gas and liquid states, FC(O)SCN and FC(O)NCS were found to exist as two conformers (C_s symmetry), in which the carbonyl double bond (C═O) adopts a synperiplanar (*syn*) and an antiperiplanar (*anti*) orientation with respect to either the SCN or NCS group. For FC(O)SCN, the conformational enthalpy difference, $\Delta H° = H°(anti) - H°(syn)$, was determined by matrix IR experiments to be 0.9 ± 0.2 kcal mol^{-1}. The conformational equilibria were evaluated by fast-cooling gaseous samples highly diluted in argon at different temperatures as cryogenic matrixes. The conformational properties of both molecules were analyzed in terms of the hyperconjugative electronic effect applying the natural bond orbital method. The kinetics of the thermal conversion of the high-energy *anti* into the *syn* FC(O)NCS conformer was studied in Ar and N_2 matrixes at cryogenic temperatures. The reversed *syn* → *anti* photoisomerization was observed using UV−vis light. Rearrangement of FC(O)SCN into FC(O)NCS was observed in the neat liquid and in solution. Under 193 nm (ArF excimer laser) irradiation, FC(O)NCS isolated in cryogenic Ar matrixes forms FC(O)SCN. At low temperature, single crystals of the two constitutional isomers were obtained using a miniature zone melting procedure. According to X-ray diffraction, they exclusively crystallize in their *syn* forms (C_s symmetry) in the orthorhombic crystal system.

Introduction

Several studies on carbonylsulfenyl compounds, $R^1C(O)SR^2$, have been carried out considering their valuable spectroscopic and electronic properties in the ground and excited states,[1−3] as well as their application as precursors in the synthesis of other covalent[4,5] and coordination[6] compounds. However, carbonyl thiocyanates, $R^2 = CN$, have not been investigated in detail, probably because they easily isomerize[7] to the more stable and well-known carbonyl isothiocyanates, $R^1C(O)NCS$.[8−12]

*To whom correspondence should be addressed. E-mail: carlosdv@quimica.unlp.edu.ar.

(1) Della Védova, C. O.; Haas, A. *Z. Anorg. Allg. Chem.* **1991**, *600*, 145–151.
(2) Erben, M. F.; Della Védova, C. O. *Inorg. Chem.* **2002**, *41*, 3740–3748.
(3) Ulic, S. E.; Della Védova, C. O.; Hermann, A.; Mack, H. G.; Oberhammer, H. *J. Phys. Chem. A* **2008**, *112*, 6211–6216.
(4) Romano, R. M.; Della Védova, C. O.; Downs, A. J.; Greene, T. M. *J. Am. Chem. Soc.* **2001**, *123*, 5794–5801.
(5) Torrico Vallejos, S.; Erben, M. F.; Boese, R.; Piro, O. E.; Castellano, E. E.; Della Védova, C. O. *J. Mol. Struct.* **2009**, *918*, 146–153.
(6) Torrico Vallejos, S. Doctoral Thesis, Universidad de la Plata, Argentina, 2009.
(7) Torrico Vallejos, S.; Erben, M. F.; Ge, M.-F.; Willner, H.; Della Védova, C. O. *J. Phys. Chem. A* **2010**, *114*, 3703–3712.
(8) Campbell, N. L.; Gillis, C. J.; Klapstein, D.; Nau, W. M.; Balfour, W. J.; Fougere, S. G. *Spectrochim. Acta* **1994**, *51A*, 787–798.
(9) Xiao, H. Y.; Xue, Y.; Xu, X. J.; Xie, D. Q.; Yan, G. S. *Acta Chim. Sin.* **2000**, *58*, 414–417.
(10) Durig, J. R.; Giurgis, G. A.; Krutules, K. A. *J. Mol. Struct.* **1994**, *328*, 55–75.
(11) Zeng, X. Q.; Yao, L.; Ge, M. F.; Wang, D. X. *J. Mol. Struct.* **2006**, *789*, 92–99.
(12) Durig, J. R.; Gamil, A. G.; Krutules, K. A. *J. Mol. Struct.* **1995**, *26*, 475–486.

Published on Web 11/08/2010

In fact, SCN ↔ NCS rearrangements are common in main-group and coordination chemistry, where this constitutional isomerism may be attributed to different mechanisms.[13−19] Basolo et al. observed in 1963 the rearrangement of $[Pd(AsPh_3)_2(SCN)_2]$ to $[Pd(AsPh_3)_2(NCS)_2]$.[13] More recently, isomerization of the kinetically favored thiocyanate form of $[Pt(SCN)_2(bpy)]$ at 25 °C in dimethyl sulfoxide (DMSO)-d_6 to the thermodynamically stable isomer $[Pt(NCS)_2(bpy)]$ through a [Pt(SCN)(NCS)(bpy)] complex was reported. This rearrangement was shown to be reversible under UV-light irradiation only in solution but not in the solid state.[16] An intramolecular 3,3 sigmatropic rearrangements through a six-membered transition state (TS) has been proposed for the constitutional isomerism of allylic thio- and isothiocyanates. In addition, ionization−recombination and bimolecular displacement reactions have also been considered.[17,18]

Hydrogen thiocyanate, HSCN, was formed by photoisomerization of hydrogen isothiocyanate, HNCS, isolated in Ar and N_2 matrixes at low temperature using 300-nm light.[19] The energy difference between HNCS and HSCN was reported to be ca. 12 kcal mol^{-1},[20] and its isomerization was attributed to the photodissociation of H···NCS, followed by hydrogen recombination. The threshold energy for the hydrogen abstraction from HNCS of 4.2 eV (294 nm), evaluated by photoionization mass spectroscopy,[21] is in agreement with the photolysis energy (300 nm).

Carbonyl thiocyanates XC(O)SCN (X = F and Cl) were synthesized by Haas and Reinke in 1967,[22] but their vibrational, conformational, and structural properties have been studied only scarcely. An early report on the rearrangement of FC(O)SCN to FC(O)NCS was based on a ^{19}F NMR study.[23] Since this time, one computational study of this isomerization using semiempirical calculations was reported.[24] The more stable FC(O)NCS was characterized by IR (gas) and Raman (liquid) spectroscopy, and the existence of two conformers due to internal rotation around the C−N bond (*syn* and *anti*) was early reported.[8] Recently, the vibrational modes of the two rotational conformers were assigned by comparison with quantum chemical results.[9]

In this work, a more detailed vibrational characterization, together with the study of the conformational and structural properties of both FC(O)SCN and FC(O)NCS, is presented. IR (gas, Ar matrix), Raman (liquid and solid), ^{13}C NMR, and UV−vis spectroscopy and single-crystal X-ray diffraction are used, complemented by quantum chemical calculations. The constitutional isomerism of FC(O)SCN to FC(O)NCS is evaluated in the gas and liquid phases using IR spectroscopy. Both isomers were isolated in solid Ar at cryogenic temperatures, and their thermal and photochemical behavior has been evaluated.

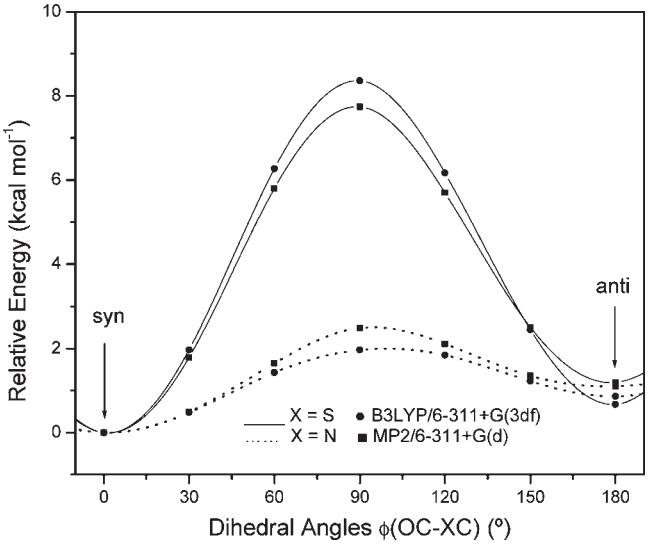

Figure 1. Potential energy curves for internal rotation around the C−X bonds in FC(O)SCN (X = S) and FC(O)NCS (X = N) calculated at the B3LYP/6-311+G(3df) (●) and MP2/6-311+G(d) (■) levels of theory.

Table 1. Relative Energies of the *Anti* Conformers of FC(O)SCN and FC(O)NCS ($\Delta E°$, Including Zero-Point Energy Corrections) and of the Internal Rotational TS [$\Delta E°$(TS)] with Respect to Their Lowest-Energy *Syn* Forms,[a] and Enthalpy ($\Delta H°$) and Free Energy ($\Delta G°$) Differences of the *Syn* and *Anti* Conformers of FC(O)SCN and FC(O)NCS, and Activation Energies for the *Anti* → *Syn* Isomerization ($E_{a,anti→syn}$) Calculated at Various Levels of Theory (at 298.15 K; in kcal mol^{-1})

method	$\Delta E°$	$\Delta H°$	$\Delta G°$	$\Delta E°$(TS)	$E_{a,anti→syn}$
FC(O)SCN					
B3LYP/6-31G(d)	0.43	0.43	0.39	7.99	7.56
B3LYP/6-311+G(d)	0.71	0.72	0.65	7.68	6.97
B3LYP/6-311+G(3df)	0.67	0.68	0.62	8.16	7.49
B3LYP/aug-cc-pVTZ	0.71	0.71	0.66	7.96	7.26
MP2/6-31G(d)	1.02	1.02	0.95	8.09	7.08
MP2/6-311+G(d)	1.19	1.20	1.08	7.55	6.36
CCSD(T)/6-311+G(d)	0.99[b]				
CBS-QB3	0.96	0.96	0.92	7.61	6.65
FC(O)NCS					
B3LYP/6-311+G(d)	0.86	0.90	0.72	1.86	1.00
B3LYP/6-311+G(3df)	0.75	0.77	0.65	1.81	1.06
B3LYP/aug-cc-pVTZ	0.72	0.75	0.62	1.73	1.01
MP2/6-311+G(d)	0.91	0.97	0.67	2.26	1.34
CCSD(T)/6-311+G(d)	1.22[b]				
CBS-QB3	0.77	0.77	0.65	1.44	0.67

[a] Absolute calculated energies of the *syn* conformers of FC(O)SCN and FC(O)NCS are shown in Table S1 (in Supporting Information). [b] Zero-point energy corrections calculated at the MP2/6-311+G(d) level of approximation.

Results and Discussion

Theoretical Calculations. The potential energy curves are shown in Figure 1 for internal rotation around the C−X (X = S and N) single bonds for FC(O)SCN and FC(O)NCS, obtained by structure optimization at fixed dihedral angles ϕ(OC−XC) from 0° to 180° in steps of 30°. Similar curves were obtained at the MP2/6-311+G(d) and B3LYP/6-311+G(3df) levels of theory, which for both compounds revealed two minima at 0° and 180°,

(13) Basolo, F.; Burmeister, J. L.; Poe, A. J. *J. Am. Chem. Soc.* **1963**, *85*, 1700–1701.
(14) Burmeister, J. L.; Basolo, F. *Inorg. Chem.* **1964**, *3*, 1587–1593.
(15) Coyer, M. J.; Herber, R. H.; Chen, J.; Croft, M.; Szu, S. P. *Inorg. Chem.* **1994**, *33*, 716–721.
(16) Kishi, S.; Kato, M. *Inorg. Chem.* **2003**, *42*, 8728–8734.
(17) Banert, K.; Hagedorn, M.; Müller, A. *Eur. J. Org. Chem.* **2001**, *2001*, 1089–1103.
(18) Kotani, M.; Shigetomi, Y.; Imada, M.; Oki, M.; Nagaoka, M. *Heteroatom Chem.* **1997**, *8*, 35–43.
(19) Wierzejewska, M.; Mielke, Z. *Chem. Phys. Lett.* **2001**, *349*, 227–234.
(20) Wierzejewska, M.; Moc, J. *J. Phys. Chem. A* **2003**, *107*, 11209–11216.
(21) Ruscic, B.; Berkowitz, J. *J. Chem. Phys.* **1994**, *101*, 7975–7989.
(22) Haas, A.; Reinke, H. *Angew. Chem.* **1967**, *6*, 705–706.
(23) Haas, A.; Reinke, H. *Chem. Ber.* **1969**, *102*, 2718–2727.
(24) Jubert, A. H.; Villar, A. H.; Castro, E. A. *J. Mol. Struct.* **1986**, *135*, 15–19.

corresponding to the *syn* and *anti* conformations, respectively. Full geometry optimization and vibrational frequencies were calculated at various ab initio [MP2 and CCSD(T)], density functional theory (DFT; B3LYP), and CBS-QB3 levels of theory to verify these minimum-energy structures and to provide zero-point vibrational energy corrections. Computed relative energies ($\Delta E°$) including zero-point energy corrections, as well as enthalpy ($\Delta H°$) and free enthalpy ($\Delta G°$) differences for the different isomers, are summarized in Table 1.

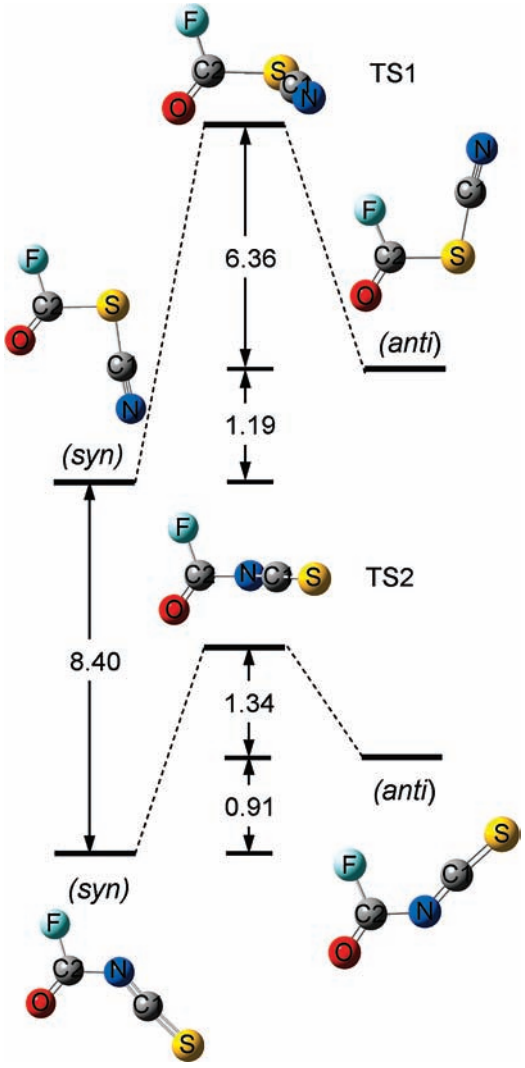

Figure 2. Optimized structures, labeling of the atoms, and relative energies of the *syn*−*anti* conformations and rotational TSs (TS1 and TS2) of the FC(O)SCN and FC(O)NCS molecules at the MP2/6-311+G(d) level of theory.

The *syn* and *anti* forms of FC(O)SCN and FC(O)NCS together with their rotational TSs and relative energies are displayed in Figure 2. Their structural parameters are listed in Tables 2 and 3, respectively. For both compounds, the *syn* form (C_s symmetry) is predicted to be lower in energy ($\Delta E°$) by 0.99 kcal mol^{-1} for FC(O)SCN and 1.22 kcal mol^{-1} for FC(O)NCS [CCSD(T)/6-311+G(d)], and from the computed $\Delta G°$, a composition of roughly 75% *syn* is predicted at room temperature for both FC(O)SCN and FC(O)NCS [B3LYP/6-311+G(3df); Table 1].

The presence of two planar minimum-energy structures and the *syn* over *anti* preference for both of these compounds can be explained in terms of lone-pair hyperconjugative effects. Natural bond orbital (NBO) calculations performed at the MP2/6-311+G(d) level reveal the presence of two lone pairs at the sulfur atom in FC(O)SCN, denoted as lp_π(S) (a″) and lp_σ(S) (a′), and occupied by 1.77 and 1.96 electrons, respectively. The lower occupancy of lp_π(S) indicates its strong electron-donor capacity. The strongest interactions are due to donations from lp_π(S) (highest occupied molecular orbital, HOMO) to both the lowest unoccupied molecular orbital (LUMO) π^*(C=O) [lp_π(S) → π^*(C=O)] and π^*(C≡N) [lp_π(S) → π^*(C≡N)]. This is evidenced by the high occupancy of the two antibonding orbitals π^*(C=O) (0.23e) and π^*(C≡N) (0.10e), which contributes to stabilization of the planar structures for FC(O)SCN by resonance (mesomeric effect). As shown in Table 4, these interactions contribute similarly to the stabilization energies for both the *syn* and *anti* forms. However, delocalization of lp_σ(S) reveals a strong conformational dependence. In account with the anomeric effect, the lp_σ(S) → σ^*(C=O) interaction stabilizes the *syn* form by 5.59 kcal mol^{-1}, while the corresponding delocalization in the *anti* form is below the threshold for printing (0.5 kcal mol^{-1}). On the other hand, the *anti* form is favored through lp_σ(S) → σ^*(C−F) delocalization by 3.71 kcal mol^{-1}. Thus, considering the electronic contributions of both lone pairs at the sulfur atom, the *syn* form is favored by 1.48 kcal mol^{-1}.

Table 2. Calculated and Experimental Structural Parameters of FC(O)SCN

	exptl[b,c]	calcd[b,d]					
		syn		anti		TS1	
parameter[a]	X-ray	B3LYP	MP2	B3LYP	MP2	B3LYP	MP2
r(C2−F)	1.340(3)	1.342	1.339	1.328	1.327	1.330	1.328
r(C2−S)	1.795(3)	1.794	1.777	1.792	1.774	1.849	1.824
r(C2−O)	1.177(4)	1.172	1.179	1.177	1.184	1.170	1.179
r(C1−S)	1.708(4)	1.691	1.688	1.692	1.689	1.689	1.688
r(C1−N)	1.136(4)	1.153	1.174	1.154	1.174	1.155	1.175
∠(F−C2−S)	106.9(2)	105.6	105.9	113.9	113.6	110.1	110.1
∠(F−C2−O)	123.6(3)	124.2	124.4	124.4	124.5	123.9	123.9
∠(O−C2−S)	129.5(3)	130.2	129.7	121.8	121.9	126.0	126.0
∠(C2−S−C1)	94.9(2)	99.2	97.3	102.8	101.4	96.6	94.4
∠(S−C1−N)	177.4(3)	174.8	175.7	175.0	175.5	176.4	177.1
ϕ(O−C2−S−C1)	0.0(1)	0.0	0.0	180.0	180.0	−88.3	−87.9

[a] For labeling of the atoms, see Figure 2. [b] Bond lengths in Å and angles in deg. [c] Error limits given in parentheses are 3σ values for the last digit. [d] The 6-311+G(3df) basis set was applied.

Table 3. Calculated and Experimental Structural Parameters of FC(O)NCS

	exptl[b,c]	calcd[b,e]					
		syn		*anti*		TS2	
parameter[a]	X-ray[d]	B3LYP	MP2	B3LYP	MP2	B3LYP	MP2
r(C2−F)	1.329(2)/1.320(2)	1.335	1.337	1.351	1.343	1.342	1.334
r(C2−N)	1.373(2)/1.366(2)	1.375	1.386	1.371	1.377	1.368	1.379
r(C2−O)	1.175(2)/1.183(2)	1.184	1.191	1.179	1.184	1.180	1.183
r(C1−S)	1.541(2)/1.538(2)	1.551	1.551	1.551	1.550	1.557	1.555
r(C1−N)	1.215(2)/1.220(2)	1.210	1.229	1.371	1.221	1.200	1.213
∠(F−C2−N)	109.6(2)/110.7(2)	109.0	108.4	111.0	110.8	110.0	109.5
∠(F−C2−O)	121.0(2)/121.0(2)	122.5	122.8	122.1	122.6	122.5	123.2
∠(O−C2−N)	129.4(2)/128.2(2)	128.5	128.8	127.0	126.6	127.5	127.2
∠(C2−N−C1)	130.8(2)/130.9(2)	136.8	131.5	138.8	136.1	147.4	140.6
∠(N−C1−S)	173.9(2)/173.8(1)	175.1	174.0	174.7	174.0	176.4	175.4
ϕ(O−C2−N−C1)	−4.6(3)/4.2(2)	0.0	0.0	180.0	180.0	−98.5	−95.3

[a] For labeling of the atoms, see Figure 2. [b] Bond lengths in Å and angles in deg. [c] Error limits given in parentheses are 3σ values for the last digit. [d] Values from the I and II nonequivalent molecules, respectively (see the X-ray Diffraction section). [e] The 6-311+G(3df) basis set was applied.

Table 4. NBO Stabilization Energies[a] for Orbital Interactions Associated with Sulfur and Nitrogen Lone Pairs in FC(O)SCN and FC(O)NCS, Respectively, Calculated at the MP2/6-311+G(d) Level of Theory

interaction	*syn*	*anti*
	FC(O)SCN	
lp_π(S) → π^*(C=O)	34.89	34.02
lp_π(S) → π^*(C≡N)	36.20	37.47
lp_σ(S) → σ^*(C=O)	5.59	
lp_σ(S) → σ^*(F−C)		3.71
$\Delta E_{anom}{}^b$	1.88	
$\Delta E_{mesom}{}^b$	−0.40	
$\Delta E_{sum}{}^b$	1.48	
$\Delta E^{\circ b}$	1.19	
	FC(O)NCS	
lp_σ(N) → σ^*(C−F)	8.62	14.43
lp_σ(N) → σ^*(C=O)	10.46	3.02
$\Delta E_{anom}{}^b$	1.63	
$\Delta E^{\circ b}$	1.10	

[a] Stabilization energies are given in kcal mol^{-1}. Threshold for printing: 0.50 kcal mol^{-1} [b] *Syn*−*anti* energy differences ΔE. Note that positive values contribute to stabilization of the *syn* rotamer. Contributions: ΔE_{anom} = anomeric interaction, ΔE_{mesom} = mesomeric interaction, $\Delta E_{sum} = \Delta E_{anom} + \Delta E_{mesom}$, ΔE° = difference of electronic energies.

Similar results were reported also for other sulfenylcarbonyl molecules.[25]

In the case of FC(O)NCS, the NBO calculations predict the presence of one σ-type lone pair at the nitrogen atom, lp_σ(N). The low occupancy (1.70e) demonstrates its high electron-donor capacity as well. It interacts mainly through the anomeric effect with σ^*(C=O) in the *syn* form [lp_σ(N) → σ^*(C=O)] but with σ^*(C−F) of the *anti* form [lp_σ(N) → σ^*(C−F)], indicating a preference of the *syn* form by 1.63 kcal mol^{-1} (Table 4).

Probably the most interesting and contrasting results uncovered by the potential energy curves shown in Figure 1 are the very different rotational barriers obtained for the two studied compounds (Table 1). Computed energy barriers E_a for the *anti* → *syn* internal rotation derived from fully optimized TS structures at various DFT and ab initio MP2 levels of theory are listed in Table 1. The TS (TS1 and TS2; Figure 2) structures were verified by an intrinsic reaction coordinate calculation to connect the conformers along the reaction path for the normal coordinate of the imaginary frequency.

An unusually low barrier of 1.34 kcal mol^{-1} [MP2/6-311+G(d)] is predicted for the *anti* → *syn* rearrangement of FC(O)NCS. A closer inspection of the corresponding internal rotation TS structure of FC(O)NCS (TS2; Table 3) calculated at the B3LYP/6-311+G(3df) level reveals a substantially wider CNC angle (147.4°) and a shorter C−NC bond length (1.368 Å) than those obtained for the *anti* (138.8°, 1.371 Å) and *syn* (136.8°, 1.375 Å) minimum-energy structures, indicating a strong variation in the hybridization of the σ-type lp_σ(N) along the reaction coordinate. On the contrary, the thiocyanate derivative cannot gain much stabilization through rehybridization of lp_σ(S) and the internal rotation TS structure is mainly destabilized by the loss of its delocalization energy associated with antibonding FC(O) orbitals.

According to calculations at the MP2/6-311+G(d) level, *syn*-FC(O)NCS is more stable than its constitutional isomer *syn*-FC(O)SCN by 8.40 kcal mol^{-1} (Figure 2). The inclusion of higher order correlation effects [CCSD(T)/6-311+G(d)] does not change this energy difference (ΔE° = 8.54 kcal mol^{-1}). In agreement with previous calculations,[24] the TS of the unimolecular isomerization of *syn*-FC(O)SCN to *syn*-FC(O)NCS was found to be nonplanar (C_1), with the SCN group perpendicular to the FC(O) moiety. Attempts to determine a planar TS structure failed. The calculated energy of the TS relative to *syn*-FC(O)NCS amounts to 62.2 kcal mol^{-1} at the MP2/6-311+G(d) level of theory. This corresponds to an activation energy E_a of 53.8 kcal mol^{-1}, which is similar to the experimental and theoretical values obtained in the related CH_3NC/CH_3CN system.[26]

Vibrational Properties of FC(O)NCS and FC(O)SCN. The vibrational spectrum of FC(O)NCS was previously described.[8,9] The gas-phase IR spectrum is shown in Figure 3 (lower trace) for comparison together with spectra of FC(O)NCS isolated in solid Ar (middle trace) and N_2 (upper trace). The latter two will be discussed below in the Matrix Isolation Experiments section.

(25) Erben, M. F.; Della Védova, C. O.; Romano, R. M.; Boese, R.; Oberhammer, H.; Willner, H.; Sala, O. *Inorg. Chem.* **2002**, *41*, 1064–1071.

(26) Liskow, D. H.; Bender, C. F.; Schaefer, H. F. *J. Am. Chem. Soc.* **1972**, *94*, 5178–5182.

Experimental and calculated frequencies for FC(O)NCS are compiled in Table 5.

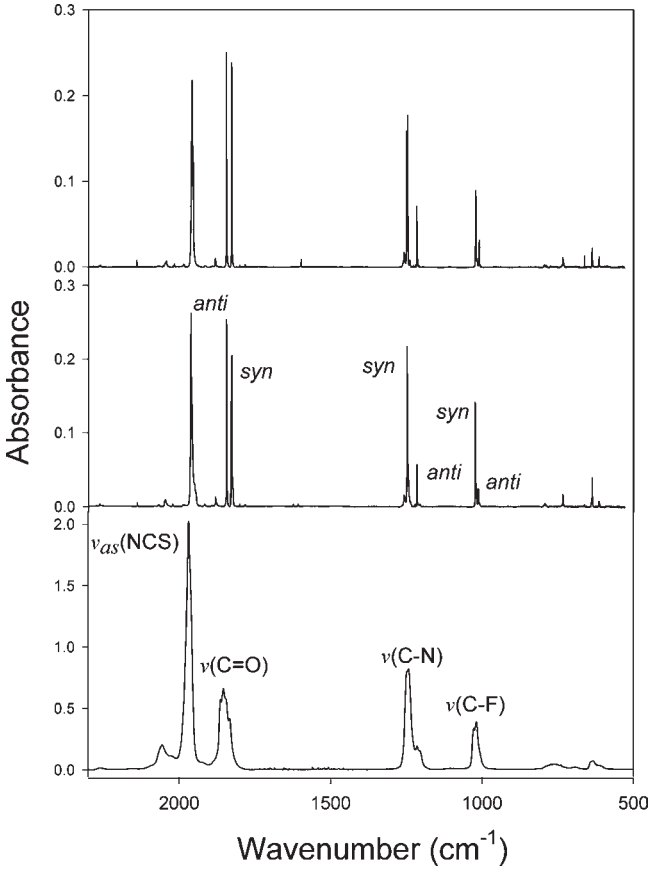

Figure 3. IR spectra of gaseous (lower trace) FC(O)NCS at 300 K, isolated in an Ar matrix (middle trace) and isolated in a N_2 matrix at 12 K (upper trace).

In Figure 4, the gas-phase IR spectrum of FC(O)SCN (lower trace) is compared with the predicted spectrum of a mixture of the *syn* (75%) and *anti* (25%) forms (upper trace), calculated at the B3LYP/6-311+G(3df) level of theory. Raman spectra of the neat liquid (lower trace) and solid FC(O)SCN (middle trace), as well as a computationally predicted spectrum of a *syn*/*anti* mixture (75%:25%, upper trace), are shown in Figure 5. Experimental band positions and relative intensities are reasonably well reproduced by the predicted spectra [B3LYP/6-311+G(3df)] of the rotamer mixture, giving confidence to the proposed

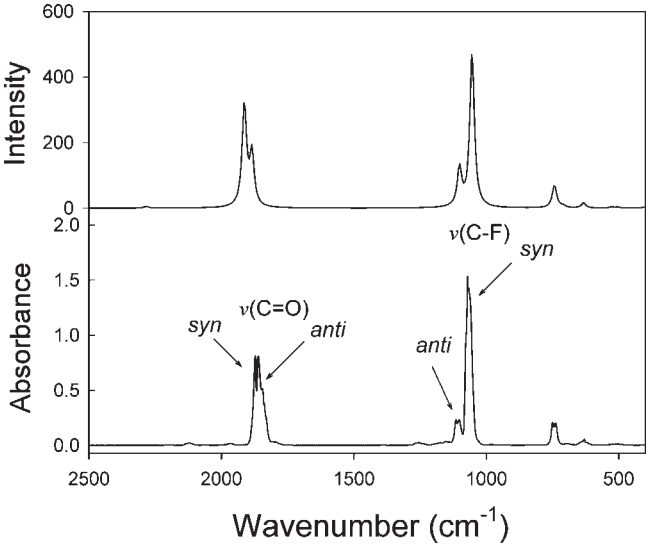

Figure 4. IR spectrum of gaseous FC(O)SCN at 300 K (lower trace) and predicted IR spectrum of a mixture of *syn*- (75%) and *anti*-FC(O)SCN (25%) calculated at the B3LYP/6-311+(3df) level (upper trace). The bands in the simulated spectrum have a Lorentzian shape, a bandwidth of 10 cm^{-1}, and an intensity in the km mol^{-1} range, and the calculated frequencies were not scaled.

Table 5. Experimental and Calculated Frequencies (cm^{-1}) and Assignment of the Vibrational Modes of FC(O)NCS

	exptl IR				calcd[e]		
mode	gas[a,b]	gas[c,b]	Ar matrix[d]	N_2 matrix[d]	*syn*	*anti*	assignment[c,f]/symmetry
	2056 w	2027 m	2045.5 (4)	2042.0			$2\nu_4$
ν_1	1969 vs	1969 vvs	1962.4	1958.5		2045 (1390)	ν_{as}(NCS)/A′
			1958.9 (100)		2044 (1549)		
			1880.2 (2)				$\nu_3 + \nu_6$
ν_2	1854 s	1863 vs	1844.3 (23)	1844.7		1890 (1066)	ν(C═O)/A′
	1837 s	1833 vs	1826.5 (23)	1826.7	1865 (503)		
			1258.7 (6)	1257.7			$2\nu_6$
ν_3	1245 s	1242 vs	1247.9 (37)	1246.1	1261 (570)		ν(C−N), ν(C−F)/A′
	1213 w	1213 m	1215.3 (5)	1215.7		1225 (275)	
ν_4	1024 m	1018 s	1022.8 (18)	1021.1	1027 (367)		ν(C−F), ν_s(NCS)/A′
	1009 w, sh		1012.2 (3)	1009.3		1007 (237)	
ν_5	760 vw, br	774 vw	793.4 (2)	795.4	795 (31)		ν_s(NCS), ν(C−N), δ(FCO)/A′
		763 vw				774 (17)	
ν_6	637 vw	617 vw	636.9 (4)	636.8	638 (55)		δ(FCO)/A′
	614 vw, sh	608 vw, sh	614.9 (1)	614.3		612 (60)	
ν_7		449 vw			475 (2)	458 (1)	δ(NCS)/A′
ν_8					443 (2)	490 (4)	δ(FCO), ν_s(NCS)/A′
ν_9					94 (1)	88 (2)	δ(CNC)/A′
ν_{10}	760 vw, br	743 vw	733.4 (2)	733.9	749 (31)		oop(FCO)/A″
		739 sh				744 (31)	
ν_{11}					494 (< 1)	489 (< 1)	oop(NCS)/A″
ν_{12}					79 (< 1)	67 (< 1)	τ (OCSC)/A″

[a] This work. [b] Band intensities: vvs, very very strong; vs, very strong; s, strong; m, medium strong; w, weak; vw, very week; sh, shoulder; br, broad. [c] Reference 8. [d] Most populated matrix site; relative intensities are given in parentheses. [e] B3LYP/6-311+G(3df)-calculated IR frequencies (cm^{-1}) and intensities (km mol^{-1}) in parentheses. [f] ν, δ, τ, and oop represent stretching, deformation, torsion, and out-of-plane modes, respectively.

assignments listed in Table 6 for the experimental and computed frequencies of *syn*- and *anti*-FC(O)SCN.

FC(O)SCN (C_s symmetry) presents nine in-plane (2N-3, A′) and three out-of-plane (N-3, A″) modes, and all of them are IR- and Raman-active. However, a distinctive feature in the Raman spectrum, which is missing in the IR spectra, is the very strong C≡N stretching mode of the SCN group located at 2187 cm^{-1} (liquid), which is easily assigned by comparison to that of related molecules (2166 cm^{-1} in CCl_3SCN,[27] 2172 cm^{-1} in CCl_2FSCN,[28] and 2189 cm^{-1} in CF_3SCN[29]).

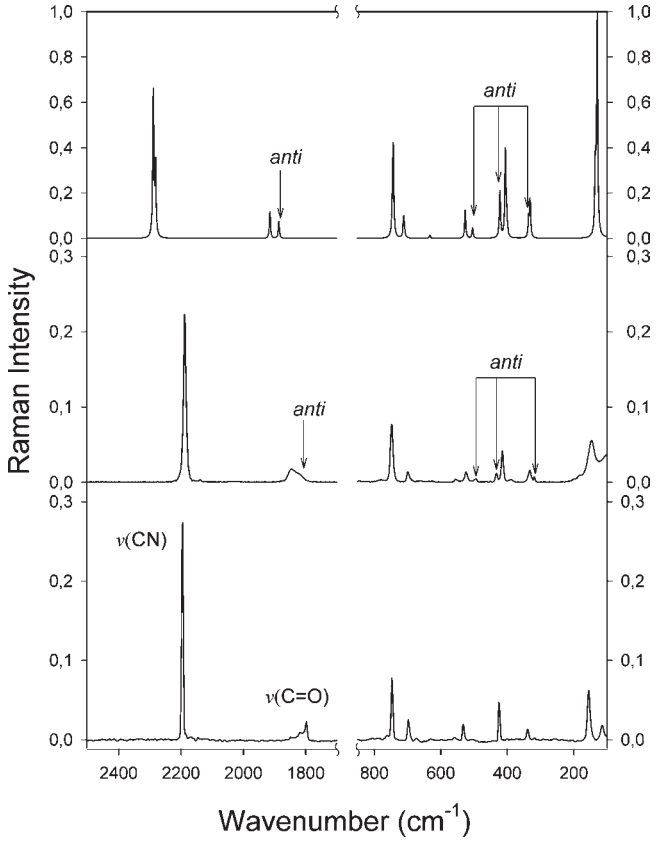

Figure 5. Raman spectra of solid FC(O)SCN at 100 K (lower trace) and liquid FC(O)SCN at 300 K (middle trace) and the predicted spectrum of a mixture of *syn*- (75%) and *anti*-FC(O)SCN (25%) calculated at the B3LYP/6-311+(3df) level (upper trace; bandwidth of 4 cm^{-1}).

In the IR gas spectrum, the characteristic C═O stretching band appeared at 1867 cm^{-1}. This mode is assigned to the more stable *syn* conformer according to its characteristic B-type band contour and quantum chemical calculations and in comparison with related compounds.[30−32] Additionally, a shoulder at 1845 cm^{-1} is clearly observed in the IR gas spectrum and assigned to the C═O stretching mode of the less stable *anti* conformer. The *syn*/*anti* wavenumber shifts $\Delta\nu$ for these modes are $\Delta\nu_{C=O}$ = 22 cm^{-1} (gas) and 18 cm^{-1} (Ar matrix). This tendency is well reproduced by the calculated values at the B3LYP/6-311+G(3df) level (28 cm^{-1}).

The bands at 1065 cm^{-1} (AB hybrid type) and 1108 cm^{-1} (gas phase) are attributed to the C−F stretching modes of the *syn* and *anti* conformers, respectively, by comparison with similar compounds [FC(O)SCl,[33] 1054 cm^{-1} (*syn*) and 1104 cm^{-1} (*anti*); FC(O)SNSO,[31] 1072 cm^{-1} (*syn*) and 1113 cm^{-1} (*anti*)]. The isomeric shifts $\Delta\nu_{C-F}$ of 43 cm^{-1} (gas) and 41 cm^{-1} (Ar matrix) are well reproduced by B3LYP/6-311+G(3df) calculations ($\Delta\nu_{C-F}$ = 48 cm^{-1}).

The C(O)−S stretching band is observed in the Raman spectra (liquid) as a medium intense feature around 746 cm^{-1} and as a weak band centered at 745 cm^{-1} (A type) in the IR gas spectra (748 cm^{-1} in FC(O)SCl[33] and 761 cm^{-1} in $FC(O)SCH_3$[32]). The S−C(N) stretching mode is attributed to the weak band at 697 cm^{-1} (liquid) and at 698 cm^{-1} (solid) in the Raman spectra. A weak band at 630 cm^{-1} in the IR gas spectrum, which exhibits the expected C-type contour, was assigned to the C═O out-of-plane mode of the *syn* conformer. This frequency is similar to the corresponding mode in *syn*-FC(O)SCl (628 cm^{-1}).[33]

Table 6. Experimental and Calculated Frequencies (cm^{-1}) and Assignment of the Fundamental Vibrational Modes of FC(O)SCN

	exptl						
	IR		Raman		calcd[c]		
mode	gas[a]	Ar matrix[b]	liquid[b]	solid	*syn*	*anti*	assignment[d] (PED)[e]/symmetry
ν_1			2187 (100)	2196	2286 (3)	2279 (5)	ν(C≡N) (93)/(A′)
ν_2	1867 s (B), ΔPR = 12	1855.7 (87)	1844 (9)	1798	1913 (306)		ν(C═O) (90)/(A′)
	1845 m, sh	1837.8 (37)				1885 (447)	
ν_3	1108 w (B), ΔPR = 12	1099.1 (53)				1101 (323)	ν(C−F) (65), δ(FCO) (20)/(A′)
	1065 vs (AB)	1058.5 (100)			1053 (466)		
ν_4	745 w (A), ΔPR = 12	742.9 (27)	746 (36)	747	742 (49)	745 (57)	δ(FCO) (48), ν(C(O)−S) (35)/(A′)
ν_5		695.9 (1)	697 (7)	698	711 (4)	709 (5)	ν(S−C(N)) (85)/(A′)
ν_6			495 (3)			504 (8)	δ(CSC) (26), δ(C(O)−S) (24), δ(SCN) (17)/ (A′)
			524 (7)	532	526 (4)		
ν_7			415 (19)	425	406 (< 1)		ν(C(O)−S) (46), δ(SCN) (21), δ(FCO) (18)/(A′)
			432 (5)			422 (< 1)	
ν_8			318 (3)			336 (< 1)	δ(FCS) (68), δ(SCN) (29)/(A′)
			332 (7)	338	331 (1)		
ν_9			146 (25)	155	130 (4)	136 (6)	δ(CSC) (54), δ(SCN) (30)/(A′)
ν_{10}	630 vw (C)	629.1 (6)			632 (11)	635 (12)	oop(FCO) (88)/(A″)
ν_{11}					403 (2)	400 (2)	oop(SCN) (93)/(A″)
ν_{12}				114	91 (2)	76 (5)	τ(OCSC) (91)/(A″)

[a] Band intensities: vs, very strong; s, strong; w, weak; vw, very week; sh, shoulder. Band-type contours are denoted in parentheses. Separation of the P- and R-type wings is denoted by ΔPR (cm^{-1}). [b] Relative intensities in parentheses. [c] B3LYP/6-311+G(3df)-calculated IR frequencies (cm^{-1}) and intensities (km mol^{-1}) in parentheses. [d] ν, δ, τ, and oop represent stretching, deformation, torsion, and out-of-plane modes. [e] Contributions (in %) to the potential energy distribution (PED) are given in parentheses.

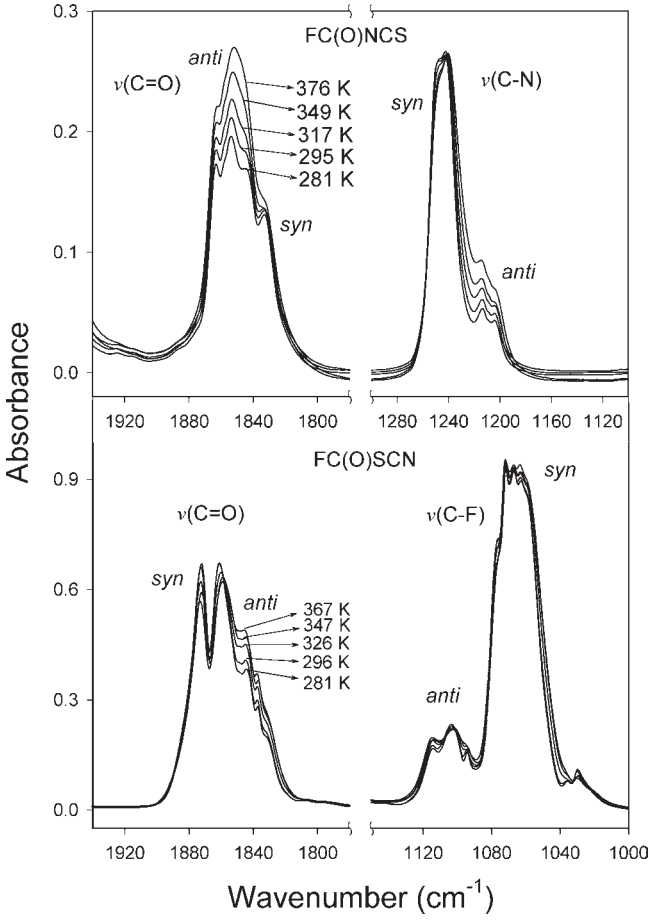

Figure 6. Part of the IR spectra of gaseous FC(O)SCN (lower trace) and FC(O)NCS (upper trace) showing the temperature dependence of the intensity of the C=O, C−F, and C−N vibrational modes.

Conformational and Constitutional Isomerism. The gas-phase IR spectrum of FC(O)SCN is consistent with the presence of a *syn* and *anti* conformer mixture, where the former one prevails. This is further proved by temperature-dependent gas-phase IR spectroscopy. Figure 6, lower trace, displays the temperature dependence of the C=O stretching band contour of FC(O)SCN recorded at different temperatures in the range from 281 to 367 K. These spectra reveal an increase in the intensities of the bands belonging to the *anti* form (1845 cm^{-1}, sh; 1108 cm^{-1}) when the cell temperature was raised, indicating the lower thermodynamic stability of this rotamer.

The equilibrium between the *syn* and *anti* conformers has also been studied in liquid FC(O)SCN. The Raman spectra of the neat liquid exhibit some weak satellite bands at 495, 432, and 318 cm^{-1}, which are assigned to the *anti* form (see the inset in Figure 5; middle trace). These bands disappear when FC(O)SCN crystallizes. Consistent with the single-crystal X-ray diffraction results (see below), only the *syn* form is observed in the Raman spectra of the solid (Figure 5, lower trace).

The existence of two conformers in the gas and liquid phases has also been reported for the constitutional isomer FC(O)NCS.[8] Our temperature-dependent IR (gas) spectra of FC(O)NCS, recorded in the range of 281−376 K, also prove the preference of the *syn* form over the *anti* form in the gas phase (Figure 6, upper trace). Similarly, as in the case of FC(O)SCN, the gas-phase absorption bands of both of these rotamers are heavily overlapped, preventing a more quantitative evaluation of the gas-phase equilibrium from these spectra.

At room temperature, FC(O)SCN is a quite unstable colorless liquid that decomposes to an orange solid [probably because of $(SCN)_x$ polymers]. Vapor-phase IR spectra revealed its rearrangement to FC(O)NCS as well as traces of additional decomposition products such as OCF_2 and OCS.

Because the vibrational frequencies of the SCN moieties in both fluorocarbonyl thio- and isothiocyanate are well separated, the kinetics of the SCN−NCS isomerization can be studied by time-dependent FTIR spectroscopy. IR spectra of completely vaporized samples of FC(O)SCN, previously distilled into a small bulb held at a certain temperature, show strong bands associated with the rearranged product FC(O)NCS (1969, 1245, and 1024 cm^{-1}; Table 5), while the intensity of the bands due to FC(O)SCN decreased with time. The time-dependent diminution of the integrated IR absorption of the C−F stretching band of FC(O)SCN (1065 cm^{-1}) was used to estimate first-order reaction rates (K) for the rearrangement of liquid FC(O)SCN into FC(O)NCS at three different temperatures. Assuming that the decomposition of FC(O)SCN to products other than FC(O)NCS is negligible in the investigated temperature range, the corresponding reaction rates (K) at 273, 303, and 328 K are 1.16×10^{-4}, 8.37×10^{-4}, and 7.24×10^{-3} s^{-1}, respectively. These K values are similar to that reported for the thoroughly investigated allyl thiocyanate to allyl isothiocyanate isomerization at 353 K in toluene (1.9×10^{-4}).[18]

However, reaction rates for the rearrangement of FC(O)SCN to FC(O)NCS are found to be strongly affected by the nature of the solvent. When the isomerization is carried out in sulfolane at 303 K (ε = 44.5), the rate constant is 1 order of magnitude higher (10^{-3} s^{-1}) than the corresponding value for the neat liquid, while the rate constant estimated from a solution of FC(O)SCN in carbon tetrachloride (ε = 2.2) was found to be 3 orders of magnitude lower (10^{-6} s^{-1}, 303 K). Correspondingly, vapor-phase IR spectra recorded from a carbon tetrachloride solution held at 303 K revealed only small changes even after 15 h (see the Supporting Information, Figure S1). Although competitive decomposition reactions affect the accuracy of the kinetic results, especially those obtained at higher temperatures in the polar solvent, they clearly verify the strong solvent dependence of the condensed-phase FC(O)SCN to FC(O)NCS rearrangement, which is nearly 10^3 times faster in sulfolane than in carbon tetrachloride.

We note that no decomposition or rearrangement was observed for gaseous FC(O)SCN even when a sample was

(27) Ulic, S. E.; Di Napoli, F.; Hermann, A.; Mack, H. G.; Della Védova, C. O. *J. Raman Spectrosc.* **2000**, *31*, 909–913.
(28) Coyanis, E. M.; Rubio, R. E.; Gobbato, K. I.; Mack, H. G.; Della Védova, C. O. *J. Mol. Struct.* **1995**, *344*, 45–51.
(29) Ben Altabef, A.; Cutin, E. H.; Della Védova, C. O. *J. Raman Spectrosc.* **1991**, *22*, 297–300.
(30) Della Védova, C. O. *J. Raman Spectrosc.* **1989**, *20*, 729–734.
(31) Romano, R. M.; Della Védova, C. O.; Boese, R. *J. Mol. Struct.* **1999**, *513*, 79–84.
(32) Della Védova, C. O. *J. Raman Spectrosc.* **1989**, *20*, 483–488.
(33) Della Védova, C. O.; Varetti, E. L.; Aymonino, P. J. *Can. J. Spectrosc.* **1982**, *28*, 107–113.

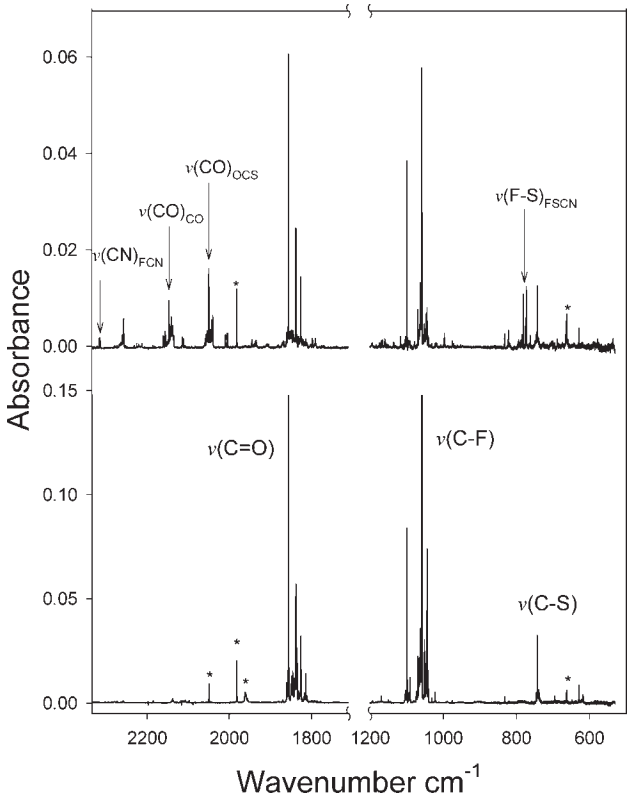

Figure 7. IR spectrum of Ar-matrix-isolated FC(O)SCN recorded before (lower trace) and after (upper trace) 13 min of photolysis using ArF excimer laser radiation (193 nm). Bands associated with impurities are denoted by asterisks.

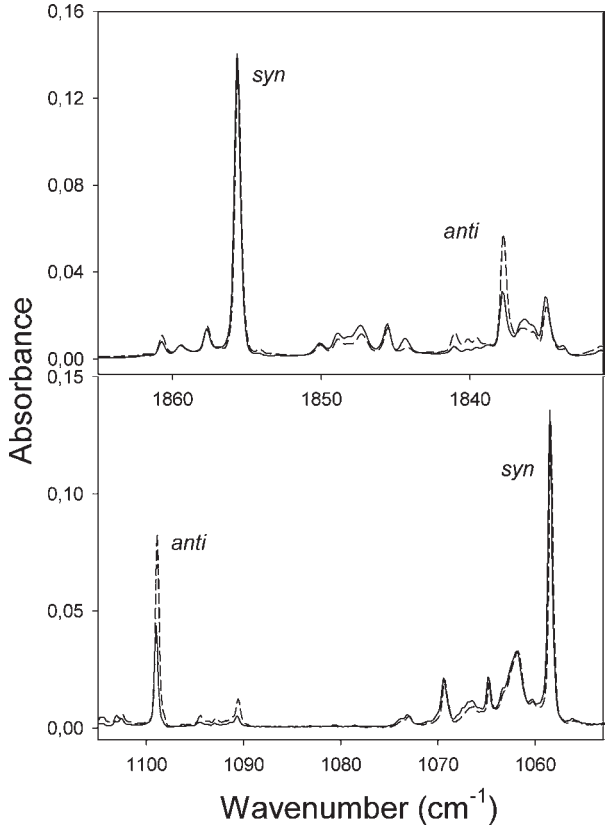

Figure 8. IR spectra in the regions of the C=O (upper trace) and C−F (lower trace) stretching fundamentals of an equilibrium mixture of *syn*- and *anti*-FC(O)SCN held at 298 K (solid line) and at 478 K (dashed line) trapped in solid Ar at 15 K. Intensities are normalized to that of ν(C=O) of *syn*-FC(O)SCN.

heated to 373 K. However, surface-catalyzed isomerization of gaseous FC(O)SCN was detected in the IR spectra recorded from mixtures of Ar and FC(O)SCN (1:4000) prepared in a stainless steel container. The observed solvent dependence is in accordance with a polar TS in a possible bimolecular S_N2 displacement reaction.[34] Such a mechanism is supported by the calculated natural and Mulliken charges for FC(O)SCN, which predict significant nucleophilic character of the terminal nitrogen atom (−0.25) in SCN and strong electrophilicity of the carbonyl carbon atom (+0.74; see the Supporting Information, Table S2).

Matrix Isolation Experiments. FC(O)SCN. The IR spectrum of FC(O)SCN isolated in solid Ar is shown in Figure 7, lower trace. Because of the sharpness of the IR absorption bands of species isolated in inert solid matrixes, the matrix isolation technique is especially suitable to study conformational equilibria. The two well-resolved C=O stretching bands of the *syn* and *anti* conformers are observed at 1855.7 and 1837.8 cm^{-1} in the Ar-matrix IR spectra (Figure 8). The C−F stretching mode of the *syn* conformer is attributed to the strongest absorption band at 1058.5 cm^{-1}, while the weaker band at 1099.1 cm^{-1} is due to the *anti* form.

Furthermore, IR spectra of deposits obtained from gaseous FC(O)SCN/Ar mixtures (1:4000) at different temperatures can be used to determine the enthalpy energy difference $\Delta H°_{exp}$ of the stable rotamers, provided that the rotational energy barrier between the two conformations is higher than ≈3 kcal mol^{-1}, which prevents a disturbance of the gas-phase equilibrium during deposition of the mixture at about 15 K.[35−37] The calculated rotational energy barrier for the *anti* → *syn* interconversion of FC(O)SCN is about 7 kcal mol^{-1} (Table 1 and Figure 1), which indicates that $\Delta H°$ might be estimated by this method. The temperature dependence of the integrated intensity ratio (K') of the two C=O bands (1855.7/1837.8 cm^{-1}; Figure 8) measured in the temperature range 298−478 K was used in a van't Hoff plot (see the Supporting Information, Figure S2). In a reasonable approximation,[37] the van't Hoff plot, expressed as $\ln K'(T) = -449.2/T\,[K] + 0.2161$, allows determination of $\Delta H°_{exp} = 0.9 \pm 0.2$ kcal mol^{-1}. This experimental value within the error limits agrees closely with the calculated ones at different levels of calculation (Table 1).

When FC(O)SCN:Ar matrixes at 15 K were exposed for 40 min to UV−vis radiation of a high-pressure Hg lamp, emitting UV−vis light (200 nm < λ < 800 nm) and equipped with a cutoff filter (Schott) transmitting light with λ > 280 nm, no change of the initial spectrum was observed. However, when using the unfiltered UV−vis

(34) Smith, P. A. S.; Emerson, D. W. *J. Am. Chem. Soc.* **1960**, *82*, 3076–3082.

(35) El-Bindary, A. A.; Klaeboe, P.; Nielsen, C. J. *J. Mol. Struct.* **1990**, *218*, 73–80.

(36) Braathen, G. O.; Gatial, A.; Klaeboe, P.; Nielsen, C. J. *J. Mol. Struct.* **1990**, *218*, 67–72.

(37) Bodenbinder, M.; Ulic, S. E.; Willner, H. *J. Phys. Chem.* **1994**, *98*, 6441–6444.

irradiation of this lamp, the relative intensities of the C=O and C−F stretching vibrations of the *anti* conformation increase at the expense of the *syn* absorptions, which reveals that a randomization process occurs. On the other hand, photolysis performed with an ArF excimer laser radiation (193 nm) results in a decrease of the IR bands of FC(O)SCN (of about 60% after 13 min) and in the appearance of new bands (Figure 7, upper trace, and Table S3 in the Supporting Information). The strongest new absorption band located at 2146.8 cm^{-1} is assigned to the CO molecule. The shift of this band relative to the pure Ar matrix isolated CO (2138.6 cm^{-1})[38] and the presence of several weak bands next to the mean absorption is attributed to the perturbation of the CO molecules because of the presence of other species formed in the same matrix cage. The second intense new band located at 2049.6 cm^{-1} could be assigned to te OCS molecule.[39,40] The photolysis products FSCN and FCN are formed as byproducts in CO and OCS formation. While the latter species gives rise to a new band appearing at 2315.8 cm^{-1}, which is close in frequency to the reported value (2316 cm^{-1}),[41] the formation of FSCN is proposed by the agreement of the attributed F−S (774.9 cm^{-1}) and S−C (688.6 cm^{-1}) stretching modes with calculated values (786 and 686 cm^{-1}, respectively) and a recent tentative experimental report (763 cm^{-1} in the Ar matrix).[42] The weaker bands of FSCN and FCN have not been observed. Although both F−S and F−N fundamental stretching modes are predicted to appear in the same region, the band observed at 774.9 cm^{-1} was not assigned to the FNCS species because the expected strong intensity of the NCS antisymmetric fundamental stretching mode was not observed.

FC(O)NCS. The IR spectrum of FC(O)NCS isolated in solid Ar and N_2 shown in Figure 3 (middle and upper traces, respectively) confirms the proposed *syn*/*anti* equilibrium in the gas phase. In fact, the most intense absorption modes present a well-resolved doublet splitting corresponding to the two rotamers. The strongest features of these doublets could be assigned to the *syn* form, because of their similar behavior in annealing experiments described below. In solid Ar, these bands are located as follows (wavenumbers in cm^{-1}): 1958.9, ν_{as}(NCS); 1826.5, ν(C=O); 1247.9, ν(C−N); 1022.8, ν(C−F); 636.9, δFC(O). The corresponding weaker bands attributed to the *anti* orientation occurred at 1962.4, 1844.3, 1215.3, 1012.2, and 614.9 cm^{-1}. The full assignment given in Table 5 agrees with that previously reported for the gas-phase spectrum.[9] IR spectra of FC(O)NCS isolated in solid N_2 are very similar to that of the Ar-matrix-isolated samples (Figure 3, upper trace), revealing only marginal matrix shifts of the observed bands, which is generally even smaller than the gas-phase to Ar-matrix shifts (Table 5).

An intriguing result of these matrix isolation spectra was that the intensity ratio between the bands of the two sets belonging to the *syn* and *anti* forms was not

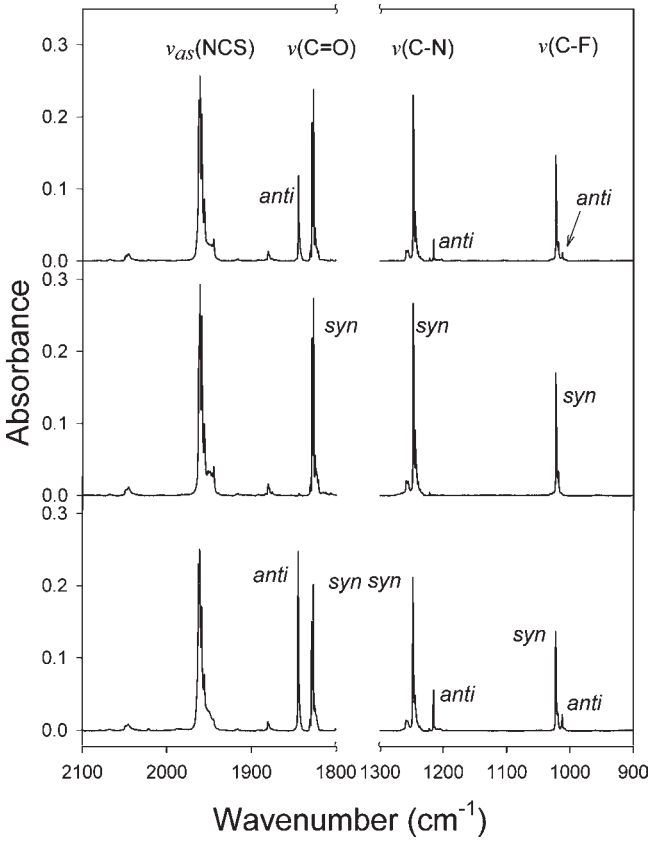

Figure 9. IR spectra of Ar-matrix-isolated FC(O)NCS at 8 K (lower trace), after annealing of the matrix to 21 K (middle trace), and after subsequent photolysis of the matrix at 8 K using a high-pressure Hg arc lamp for 5.5 min (upper trace).

reproduced in repeated measurements at the usual deposition temperatures (~15 K), indicating a perturbation of the gas-phase equilibrium composition during matrix deposition. This effect is not unexpected for conformers characterized by a very low rotational barrier (< 3 kcal mol^{-1}).[35−37] The *anti* → *syn* internal rotational barrier of FC(O)NCS is calculated to be around 1.3 kcal mol^{-1} [MP2/6-311+G(d)]. Such a small barrier may not allow a sudden trapping without a change in the gas-phase equilibrium composition, and depending on the deposition conditions, an enhancement of the more stable *syn* rotamer was observed. Furthermore, when the Ar matrix was held at 15 K, the intensity of the bands due to the more stable *syn* conformer increased with time at the expense of those of the *anti* form (see the Supporting Information, Figure S3), and when the temperature of the Ar matrix was shortly raised to 21 K, all of the bands assigned to the *anti* rotamer disappeared completely (Figure 9, middle trace). On the other hand, no *anti* → *syn* rearrangement was observed, and reproducible Ar-matrix spectra were obtained when the deposition was carried out at temperatures lower than 12 K.

The preliminary experiments proved the conformational equilibrium between *syn*- and *anti*-FC(O)NCS to be particularly useful for kinetic studies under matrix isolation conditions. Ar and N_2 matrixes are known to be rigid enough to prevent diffusion and aggregation at temperatures up to 30 and 35 K, respectively,[43] and, consequently, they are suitable "solid hosts" for kinetic

(38) Dubost, H. *Chem. Phys.* **1976**, *12*, 139–151.
(39) Verderame, F. D.; Nixon, E. R. *J. Chem. Phys.* **1966**, *44*, 43–48.
(40) Lang, V. I.; Winn, J. S. *J. Chem. Phys.* **1991**, *94*, 5270–5274.
(41) Jacobs, J.; Willner, H.; Pawelke, G. *J. Phys. Chem.* **1992**, *96*, 5793–5796.
(42) Pasinszki, T.; Bazsó, G.; Krebsz, M.; Tarczay, G. *Phys. Chem. Chem. Phys.* **2009**, *11*, 9458–9467.

Table 7. Rate Constants (K), Half-Life Times ($t_{1/2}$), and Activation Energies (E_a) for the *Anti* → *Syn* Rotational Isomerization of FC(O)NCS in Solid Ar and Solid N_2

T (K)	K ($\times 10^{-4}$ s^{-1})	$t_{1/2}$ (min)	E_a (kcal mol^{-1})
	Ar Matrix		
14.0	1.9 ± 0.2	62	
14.5	2.2 ± 0.3	51	
15.2	5.0 ± 0.2	23	0.26 ± 0.04
16.1	8.9 ± 0.5	13	
18.0	12.5 ± 0.6	9	
	N_2 Matrix		
13.5	2.9 ± 0.1	39	
14.0	5.2 ± 0.2	22	
14.6	8.7 ± 0.3	13	0.53 ± 0.05
15.0	24.2 ± 1.0	5	
15.5	34.9 ± 2.0	3	

experiments in the temperature range from 12 to 21 K. The conversion of the less stable *anti* conformer into the *syn* form is slow at temperatures of around 14 K and was followed by monitoring the change of their respective C═O absorptions located at 1844.3/1844.7 cm^{-1} and 1826.5/1826.7 cm^{-1} in the Ar/N_2 matrixes, respectively. The kinetic results are summarized in Table 7. The rate constants, K, obtained from the first-order decay of the integrated absorption I of the *anti* form according to the equation $\ln(I_t/I_0) = -K(t)$ were found to be slightly higher in the N_2 matrix than in the Ar matrix. The energy barrier, E_a, for the *anti* → *syn* isomerization, calculated using the Arrhenius equation $\log K = -E_a/2.303RT + \log A$ (A = Arrhenius preexponential factor), yields E_a = 0.26 ± 0.04 kcal mol^{-1} for the Ar matrix (14.0−18.0 K) and E_a = 0.53 ± 0.05 kcal mol^{-1} in solid N_2 (13.5−15.5 K).

The observed dependence of the rotamer interconversion on the nature of the matrix is probably due to different sample−matrix interactions. The *anti* → *syn* isomerization becomes faster and the energy barrier is found to be higher in the N_2 matrix. This result is explained by the appreciably different Arrhenius preexponential factors, which were found to be larger for the N_2 matrix ($\log A$ = 5.1) than for the Ar matrix ($\log A$ = 0.3) by about 5 orders of magnitude. The preexponential factors are related to the entropy of the system and strongly influenced by the solid hosts. It is well-known that the mobility of a trapped molecule in its cage depends to a large extent on the cage size and its structure, which varies with the nature of the matrix. This was also evidenced by the preexponential factor of $\log A$ = 11.2 determined for the cis → trans conversion of methyl vinyl ketone in a CCl_4 matrix in the temperature range of 60−70 K (E_a = 17.6 kcal mol^{-1}).[43]

After annealing of the Ar matrix to 21 K and the almost complete *anti* → *syn* rearrangement, the reversed *syn* → *anti* interconversion at temperatures lower than 12 K was achieved upon exposure of the deposit to broad-band UV−vis radiation, as shown in Figure 9 (upper trace). The simultaneous increase of all absorption bands of the *anti* conformer at the expense of the bands due to the *syn* form during photolysis is the consequence. In this photochemical isomerization, equilibrium is reached by excitation of the *syn* rotamer to a level above the internal rotation barrier and subsequent relaxation ending up in the lowest-energy state of the *anti* rotamer.

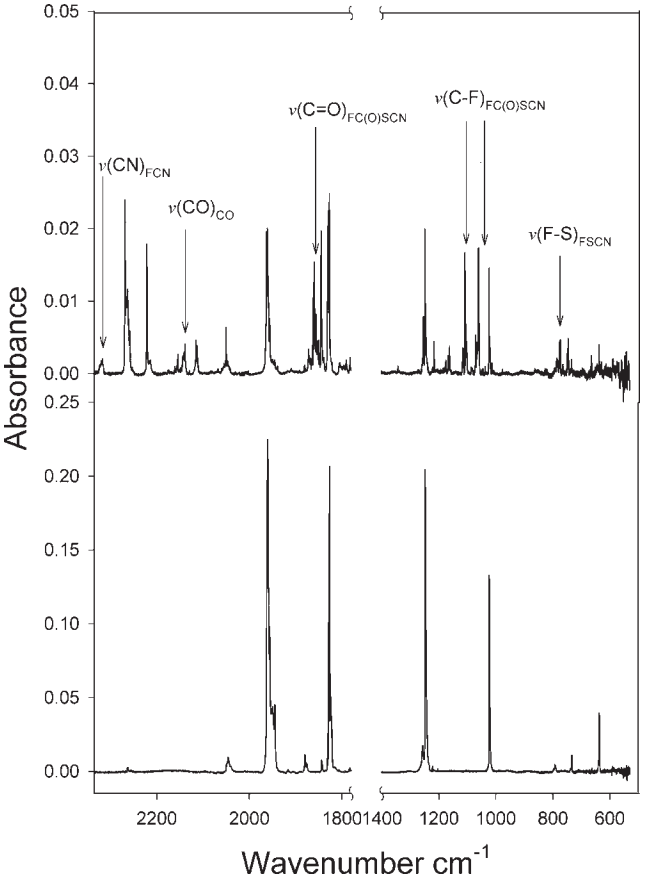

Figure 10. IR spectrum of Ar-matrix-isolated FC(O)NCS recorded before (lower trace) and after (upper trace) 5 min of photolysis using an ArF excimer laser (193 nm).

On the other hand, photolysis performed with ArF excimer laser radiation (193 nm) results in decomposition of FC(O)NCS (about 90% after 5 min), and some weak new bands appeared in the spectrum (Figure 10 and Table S4 in the Supporting Information). Most of these bands revealed site splitting, and some of the new bands of the photoproducts could not be assigned conclusively (see the Supporting Information, Table S4). However, photodecomposition yields CO (2138.8 cm^{-1}) and FSCN, a possible byproduct of CO formation that was assigned to a weak band observed at 774.9 cm^{-1} [ν(F−S)] according to theoretical predictions.[44]

Additionally, two new bands at 2316.8 and 1084.8 cm^{-1} are tentatively assigned to FCN according to literature data.[41] Furthermore, the spectrum obtained from the photolysis products clearly indicates the photochemical conversion of some FC(O)NCS in both of the two conformers of the thermodynamically less stable constitutional isomer FC(O)SCN: *syn*-FC(O)SCN [ν(C═O) = 1855.7 cm^{-1}] and *anti*-FC(O)SCN [ν(C═O) = 1837.8 cm^{-1}; ν(F−C) = 1099.0 cm^{-1}]. The F−C absorption of *syn*-FC(O)SCN (1058.5 cm^{-1}) appeared to be obscured by a hitherto unknown product band located at 1059.3 cm^{-1}.

The rich chemistry induced by irradiation ($h\nu$) and annealing (Δ) of FC(O)SCN and FC(O)NCS isolated in

(43) Pong, R.; Goldfarb, T. D.; Krantz, A. *Ber. Bunsenges Phys. Chem.* **1978**, *82*, 9–10.

(44) Durig, J. R.; Zheng, C.; Deeb, H. *J. Mol. Struct.* **2006**, *784*, 78–92.

Scheme 1. Summary of the Annealing (Δ) and Photochemical (*hν*) Isomerization Reactions, as well as of the Photodecomposition Observed for FC(O)SCN and FC(O)NCS Isolated in Solid Ar[a]

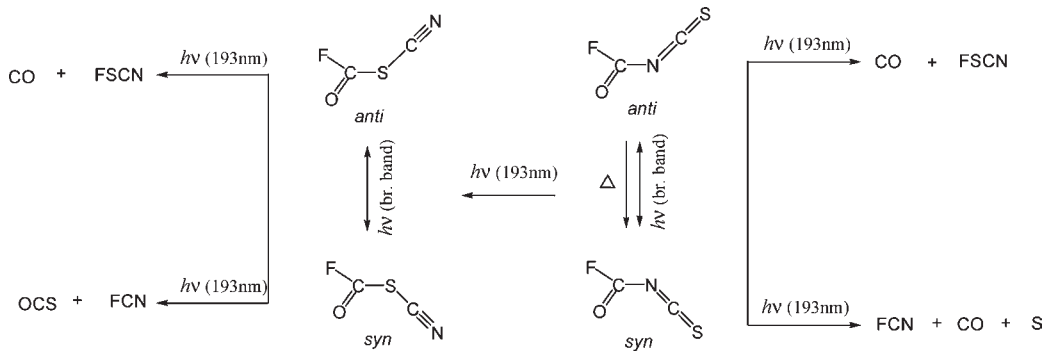

[a] br-band represents broad band (200 nm $< \lambda <$ 800 nm).

Scheme 2. Four-Dimensional Representation of Relevant Hypersurface Coordinates for FC(O)SCN−FC(O)NCS Isomerism and Conformational System in Some Electronic Ground and Excited States

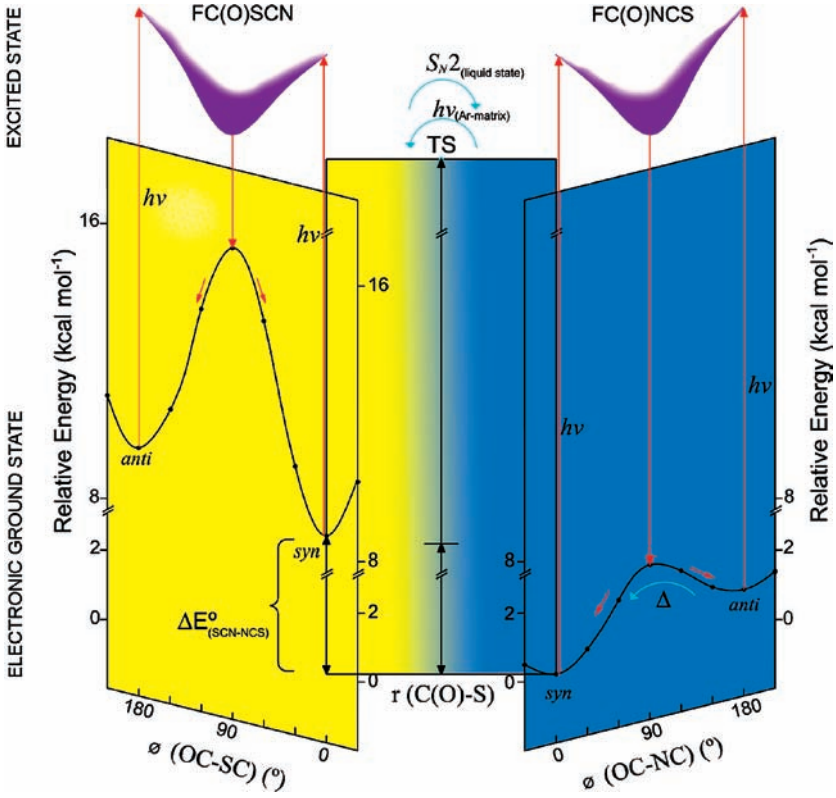

Ar and N_2 matrixes, together with a schematic four-dimensional representation of the relative energies between the conformational equilibrium, are summarized in Schemes 1 and 2.

Single-Crystal X-ray Diffraction. Crystals of FC(O)SCN and FC(O)NCS were grown in situ at 150 K in thin capillaries. The full crystallographic and refinement data of both compounds have been deposited with the Cambridge Crystallographic Data Centre (see the Experimental Section).

FC(O)SCN. Fluorocarbonyl thiocyanate crystallizes in the orthorhombic system [space group *Pnma* (No. 62)] with four FC(O)SCN molecules in the unit cell [a = 11.407(3) Å, b = 5.7551(19) Å, and c = 5.9750(19) Å]. The molecular structure is shown in Figure 11. The main geometric parameters derived from the structure refinement and those obtained from quantum chemical calculations are listed in Table 2. The representation of the crystal packing is shown in Figure 12.

The molecule exhibits crystallographic C_s symmetry, which forces a dihedral angle ϕ(O−C2−S−C1) = 0.0°. Because no indication was observed for any F/O disorder, it is concluded that solid FC(O)SCN exists exclusively as the *syn* rotamer. The molecules are arranged in alternating layers with the molecular skeletons parallel to the *ac* crystallographic plane, which are separated from each other by approximately 2.85 Å. Moreover, each layer is formed by staggered "rows" of molecules where the SCN group points in opposite directions. This molecular arrangement seems to stabilize the molecular layers by

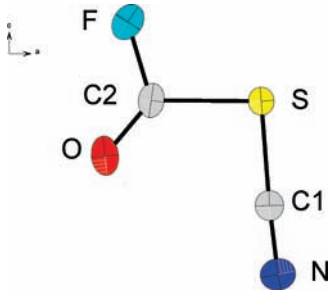

Figure 11. View of the FC(O)SCN molecule. Thermal ellipsoids are drawn at the 50% probability level.

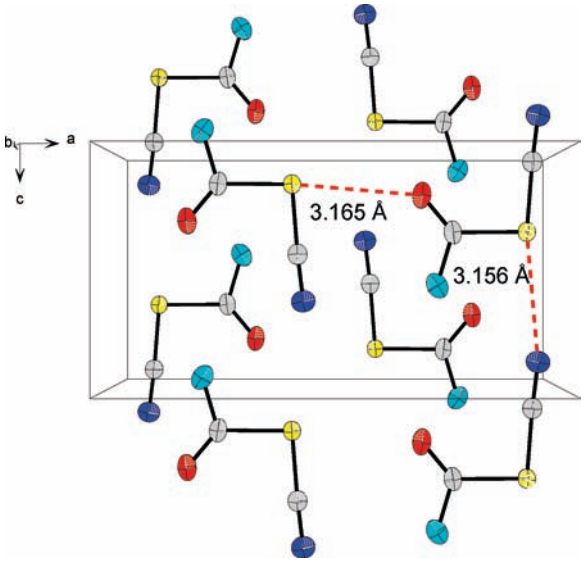

Figure 12. View of the unit cell of FC(O)SCN along the *b* axis. Thermal ellipsoids are drawn at the 50% probability level.

intermolecular interactions of the sulfur atom with the proximal nitrogen atom of the thiocyanate moiety located in the same "row" and with the oxygen atom of the carbonyl group of the next "row", where the nonbonded distances between S−C≡N···S−C≡N (parallel to the *c* axis) and C=O···S−C≡N (perpendicular to the *c* axis) are 3.156 and 3.165 Å, respectively. These distances are shorter than the sum of the van der Waals radii for sulfur and nitrogen (3.35 Å) and for sulfur and oxygen (3.32 Å)[45] (Figure 12).

The structural parameters are well reproduced by those derived from quantum chemical calculations (see Table 2). The calculated bond distances are better reproduced by the B3LYP/6-311+G(3df) method than the MP2/6-311+G(3df) method and show a maximum deviation of 0.02 Å at the overestimated C≡N bond. The deviation in the angle values is quite high but lower with the MP2/6-311+G(3df) method, which overestimates the C2−S−C1 angle by 2.4° and predicts a minor value for the S−C1−N angle by 1.7°. However, it is, in principle, reasonable considering that the calculations are performed for the molecule in the gas phase, where the intermolecular interactions observed in the crystal lattice are not taken into account. Additionally, the structural parameters obtained by X-ray diffraction of molecules

(45) Bondi, A. *J. Phys. Chem.* **1964**, *68*, 441–451.

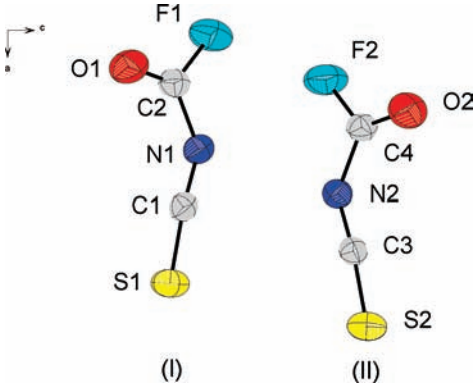

Figure 13. View of the two crystallographic nonequivalent FC(O)NCS molecules. Thermal ellipsoids are drawn at the 50% probability level.

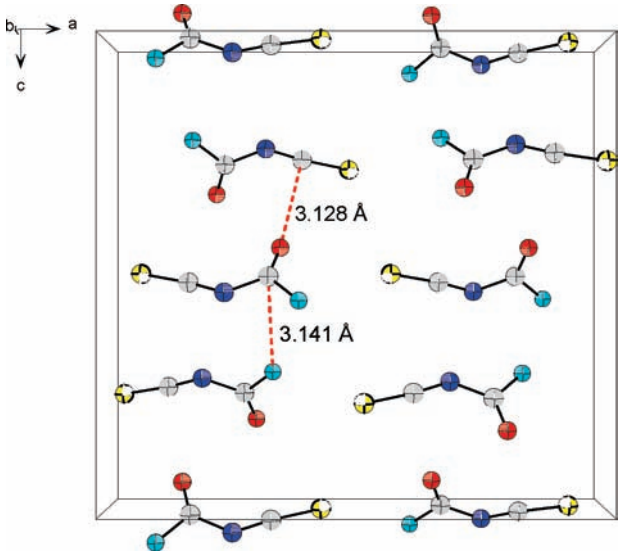

Figure 14. View of the unit cell of FC(O)NCS along the *b* axis. Thermal ellipsoids are drawn at the 50% probability level.

that own the FC(O) and SCN groups like FC(O)SCl[46] and CH_2ClSCN[47] show values similar to those obtained for FC(O)SCN.

FC(O)NCS. Fluorocarbonyl isothiocyanate crystallizes in the orthorhombic system [space group $Pca2_1$ (No. 29)] with eight FC(O)NCS molecules in the unit cell [a = 14.784(2) Å, b = 3.9255(6) Å, and c = 13.918(2) Å]. Two crystallographic nonequivalent molecules (I and II) of FC(O)NCS form the unit cell and are shown in Figure 13. The main geometric parameters derived from the structure refinement and those obtained from quantum chemical calculations are listed in Table 3. The representation of the crystal packing is shown in Figure 14.

Only the most stable *syn* conformer of FC(O)NCS is observed in the single crystal, similar to FC(O)SCN. However, the *syn*-FC(O)NCS structure is slightly distorted from the C_s symmetry [dihedral angles ϕ(O1−C2−N1−C1) = −4.6(3)° and ϕ(O2−C4−N2−C3) = 4.2(3)°]. The molecules are arranged in alternating "layers" of the

(46) Romano, R. M.; Della Védova, C. O.; Boese, R. *J. Mol. Struct.* **1999**, *513*, 101–108.

(47) Pirani, L. R.; Erben, M. F.; Boese, R.; Della Védova, C. O. Manuscript in preparation.

two nonequivalent molecules along the *ab* crystallographic plane. Each molecule interacts with three nonequivalent molecules located in the next "layers" by intermolecular O1···C3 and O2···C1 contacts of the carbonyl and isothiocyanate groups. These contacts have distances between of 3.156 and 3.101 Å, respectively. Moreover, the fluorine atom of the nonequivalent molecule II and the carbonyl group of molecule I have a C2···F2 nonbonded distance of 3.141 Å, all of which are shorter than the sum of the van der Waals radii for oxygen and carbon (3.22 Å) and for fluorine and carbon (3.17 Å)[45]. These electrostatic interactions and the smaller energy requirements for deformation of the dihedral angle ϕ(O−C−N−C) (see Figure 1) could be responsible for deviation of this molecule from the C_s symmetry.

The structural parameters are well reproduced by theoretical calculations (see Table 3). However, the distances are better predicted by the B3LYP/6-311+G(3df) approximation, with a maximum error of 0.01 Å in the overestimation of the C1−S1 and C2−F1 bond distances. On the other hand, the angles are better reproduced by the MP2/6-311+(3df) method especially for the C2−N1−C1 angle, which is predicted to be only 0.6° larger than the experimental value of 131°, in contrast to the CBS-QB3 and B3LYP/6-311+G(3df) methods, which overestimate this value by 5.2° and 5.9°, respectively. All calculations predict C_s symmetry and torsion angle values of ϕ(O1−C2−N1−C1) = 0.0° for the *syn* rotamer, which differ from experimental values by about 4.4°. However, this deviation is acceptable, as observed and commented upon in the case of FC(O)SCN.

Conclusion

This work presents the synthesis and a full structural and spectroscopic characterization of the fluorocarbonyl pseudohalides FC(O)SCN and FC(O)NCS. The two constitutional isomers were shown to exist in a *syn*/*anti* equilibrium in the gas and liquid phases according to their vibrational spectra (IR and Raman). The observed preference of the *syn* forms of the two studied compounds is in accordance with the anomeric effect and might be explained by considering mainly donor−acceptor interactions associated with the sulfur and nitrogen lone pairs, respectively. However, low-temperature single-crystal X-ray diffraction and solid-state Raman spectroscopy demonstrate the existence of only the more stable *syn* conformer in the solid state of the investigated pseudohalides.

In close agreement with the theoretical predictions, the syn − *anti* enthalpy difference for FC(O)SCN was determined to be $\Delta H°_{exp} = 0.9 \pm 0.2$ kcal mol^{-1} by trapping of the temperature-dependent gas-phase equilibrium composition in a solid Ar matrix at 15 K. Broad-band UV−vis irradiation of the Ar-isolated FC(O)SCN at cryogenic temperatures leads to the *syn*/*anti* randomization process.

A fast *anti* → *syn* interconversion was observed for FC(O)NCS isolated in solid Ar and N_2 matrixes at 13−21 K. The corresponding exchange rate for the internal rotation around the C−N bond revealed an important dependence on the nature of the matrix due to largely unknown sample−matrix interactions. From the temperature dependence of these exchange rates, the barrier for the *anti* → *syn* rearrangement was estimated to $E_a = 0.26 \pm 0.04$ kcal mol^{-1} for the Ar matrix (14.0−18.0 K) and $E_a = 0.53 \pm 0.05$ kcal mol^{-1} in solid N_2 (13.5−15.5 K). The reversed *syn* → *anti* interconversion was observed by exposure of the Ar-matrix-isolated sample at 12 K to UV−vis radiation.

Liquid FC(O)SCN is unstable at room temperature and isomerizes to FC(O)NCS. The strong solvent dependence of the corresponding reaction rates suggests a bimolecular displacement (S_N2) reaction via a polar TS. ArF laser irradiation (193 nm) of Ar-matrix-isolated FC(O)NCS causes its decomposition to CO, FCN, and FSCN, as well as some photoisomerization to the thermally less stable constitutional isomer FC(O)SCN.

Solid FC(O)SCN adopts an overall C_s symmetry. The very small barrier to internal rotation around the C−N bond and intermolecular interactions might be responsible for the slightly distorted C_s molecular symmetry of FC(O)NCS in the solid.

Experimental Section

Synthesis. FC(O)SCN was synthesized by the reaction of fluorocarbonylsulfenyl chloride, FC(O)SCl, and an excess of silver cyanide, AgCN, according to a literature procedure[23] with some modifications. The reaction was carried out in vacuum for 45 min at 273 K. The purification of the product was performed by repeated trap-to-trap distillations at trap temperatures held at 223, 183, and 77 K. FC(O)SCN isolated in the trap at 223 K contained small amounts of its constitutional isomer, FC(O)NCS, from which the more volatile FC(O)NCS was further separated by slow vacuum distillation. The final yield was around 60%.

FC(O)NCS was prepared by the reaction of fluorocarbonyl chloride, FC(O)Cl, and an excess of silver thiocyanate, AgSCN. FC(O)Cl (20 mmol) was distilled onto dry AgSCN (30 mmol) in a vessel provided with a Young valve. The mixture was kept at 273 K for 5 days in a Julabo F25-ME cryostat, and then the products were separated by trap-to-trap distillation, keeping the traps at 223, 178, and 77 K. FC(O)NCS was retained in the 178 K trap together with a small amount of FC(O)Cl, which was removed by slow vacuum distillation. The yield was around 30%.

The purities of FC(O)SCN and FC(O)NCS were checked by IR, Raman, UV, and (^{19}F, ^{13}C) NMR spectroscopy (see below).

Physical Properties and Spectroscopic Characterization. FC(O)SCN is a colorless liquid at room temperature and thermally unstable at ambient conditions. The white solid melts at 233 K, and the vapor pressure over the temperature range 238−280 K follows the equation $\ln p_v$[mbar] = −2837.55/T[K] + 13.13. The extrapolated boiling point amounts to 457 K. The ^{19}F NMR spectrum (δ = −50.2 ppm) was in accordance with previous measurements.[23] The ^{13}C NMR spectrum of FC(O)SCN exhibits two doublets (see the Supporting Information, Figure S4). The chemical shift δ and the coupling constant ^1J(CF) of the carbonyl carbon signal [δ = 153.7 ppm, ^1J(CF) = 374.5 Hz] agree well with reported values for FC(O) compounds.[25,30−32] The carbon signal associated with the SCN group is located at δ = 104.8 ppm [^3J(CF) = 6.8 Hz]. The UV−vis spectrum of FC(O)SCN exhibits one strong absorption band at 198 nm (see the Supporting Information, Figure S5), which is attributed to the $\pi \rightarrow \pi^*$ transition of the C=O chromophore by comparison with similar compounds.[1]

The IR (gas) and Raman (liquid) spectra of FC(O)SCN are shown in Figures 4 and 5, respectively. Observed bands are compiled in Table 6 together with a tentative assignment. The intense bands at 1867 and 1065 cm^{-1} are assigned to the ν(C=O) and ν(C−F) of the FC(O) group, respectively. The characteristic CN stretching band is observed in the Raman (liquid) spectrum at 2187 cm^{-1}.

FC(O)NCS is a colorless liquid at room temperature, and it is temperature- and moisture-sensitive. The melting point (200 K),

extrapolated boiling point (337 K), and ^{19}F NMR spectrum ($\delta = -16.0$ ppm) have previously been reported.[23] The ^{13}C NMR spectrum of FC(O)NCS shows two doublets at $\delta = 154.7$ ppm [^{3}J(CF) = 17.3 Hz] and $\delta = 138.6$ ppm [^{1}J(CF) = 299.1 Hz], which correspond to the carbon atoms of the NCS and C=O groups, respectively (see the Supporting Information, Figure S6). The UV−vis spectrum shows two absorptions, one appears below 190 nm and the much weaker second band at 260 nm. These absorptions are assigned by comparison with related molecules[48] to the $\pi \rightarrow \pi^*$ and $n_s \rightarrow \pi^*$ transitions within the C=O and NCS groups, respectively (see the Supporting Information, Figure S5). The IR (gas; Figure 3) and Raman (liquid) spectra are in agreement with those in previous reports.[8]

Isomerization Experiments. The rearrangement of fluorocarbonyl thiocyanate, FC(O)SCN, into fluorocarbonyl isothiocyanate, FC(O)NCS, was studied in the gas and liquid phases. For the gas-phase experiments, 2 mbar of FC(O)SCN was placed in an IR gas cell and kept at room temperature (298 K). IR spectra were recorded at different times (0−14 h) to monitor the isomerization. For liquid-phase studies, small amounts of FC(O)SCN (5 mg) were condensed in a small vessel adapted to a vacuum line, which was connected to an IR gas cell. This vessel was kept at 273 K, and IR spectra of vaporized samples were recorded at different times (0−270 min). This procedure was repeated at 303 K (0−120 min) and at 328 K (0−10 min). Additionally, to verify any influence of the solvent polarity on the isomerization process, experiments were carried out at 303 K using various solvents of different relative permittivity (ε_r) such as sulfolane (0−10 min), acetonitrile (0−60 min), and carbon tetrachloride (0−15 h).

Instrumentation. a. General Procedure. Volatile materials were manipulated in a glass vacuum line equipped with a capacitance pressure gauge (221 AHS-1000, MKS Baratron, Burlington, MA) and three U-traps and valves with PTFE stems (Young, London, U.K.). The vacuum line was connected to an IR cell (optical path length 200 mm; Si windows 0.5 mm thick) placed in the sample compartment of a Bruker Vector 25 FTIR spectrometer. This arrangement allowed one to follow the course of the reactions and the purification processes. The pure compounds were stored in flame-sealed glass ampules under liquid nitrogen in a Dewar vessel. The ampules were opened with an ampule key[49] at the vacuum line, an appropriate amount was taken out for the experiments, and then they were flame-sealed again. The vapor pressures of the samples were measured in a small vacuum line equipped with a calibrated capacitance pressure gauge (AHS-100, MKS Baratron) and a small sample reservoir. The melting points were determined using small amounts of the samples contained in a 4 mm glass tube immersed in a cold bath in a transparent Dewar vessel.

b. Vibrational Spectroscopy. IR gas spectra were recorded on a Bruker Vector 25 spectrometer, with a resolution of 2 cm^{-1} in the range from 4000 to 400 cm^{-1}, using a glass cell with Si windows and an optical path length of 200 mm.

Temperature-dependent IR spectra were measured on a Bruker IFS 66v/S FTIR spectrometer (resolution: 2 cm^{-1}) using a KBr beam splitter and a mercury−cadmium−telluride (MCT) detector in the region of 5000−530 cm^{-1}. For this purpose, a double-walled gas cell with an optical path length of 200 mm, equipped with Si windows (0.5 mm thick), a pressure gauge (221 AHS-100, MKS Baratron, Burlington, MA), and a Pt-100 temperature sensor, was placed in the evacuated sample compartment of the spectrometer. The temperature was controlled by cold and warm nitrogen gas streams at high flow rates. Up to five IR spectra at different temperatures in the range from 281 to 367 K were recorded for gaseous FC(O)SCN and FC(O)NCS. For each of these temperatures, the cell was refilled with a new sample and a new background was recorded.

Raman spectra of the neat liquid (room temperature) and of solid samples (cooled with nitrogen gas) were measured in flame-sealed capillaries (3 mm o.d.) on a Bruker RFS 106/S spectrometer, equipped with a 1064 nm Nd:YAG laser, in the region from 4000 to 100 cm^{-1} at a resolution of 2 cm^{-1}.

c. Matrix Isolation Experiments. For matrix isolation experiments performed at Wuppertal University, a few milligrams of FC(O)SCN were transferred to a small U-trap connected to the inlet nozzle of the matrix apparatus. A gas stream of argon (2 mmol h^{-1}) was directed over the sample held at 178 K, and the resulting gas mixture was condensed onto the cold matrix support (15 K, Rh-plated Cu block) in a high vacuum. The thermally more stable FC(O)NCS was mixed with argon (or nitrogen) in a ratio of 1:4000 in a 1 L stainless-steel storage container, and then small amounts of the mixture were deposited within 10 min onto the cold matrix support (lower than 12 K).

Temperature-dependent experiments were carried out by passing the gaseous sample−Ar mixtures through a quartz nozzle (1 mm i.d.), heated over a length of ≈10 mm with a platinum wire (0.25 mm o.d.) prior to deposition on the matrix support. The nozzle was held at 373 and 478 K for FC(O)SCN and at 373 and 463 K for FC(O)NCS. Photolysis experiments were performed using an ArF excimer laser (193 nm, Lambda-Physics) and exposure times of 13 min (2 mJ and 5 Hz repetition time) for FC(O)SCN and 5 min (3 mJ and 5 Hz) for FC(O)NCS. High-pressure Hg lamp (TQ 150, Heraeus) radiation passed through water-cooled quartz lenses, various filters, and an outer quartz window at the cryostat was also used in the photolysis experiments. For FC(O)SCN (10 and 40 min), a cutoff filter (Schott, >280 nm) was employed, while FC(O)NCS was irradiated through a 255 nm interference filter (Schott) for 13 and 30 min.

IR spectra of matrix-isolated samples were recorded in reflectance mode on a Bruker IFS 66v/S spectrometer using a transfer optic. An MCT detector, a KBr/Ge beam splitter, and a CsI window at the cryostat were used in the wavenumber range 5000−530 cm^{-1}. For spectra with apodized resolutions of 0.25 cm^{-1} and 200 scans, a few scans in the annealing measurements were added. More details of the matrix apparatus are given elsewhere.[50]

Annealing experiments were performed on deposits of FC(O)NCS isolated in solid Ar and N_2. The deposits were prepared as described above and at temperatures lower than 12 K. The deposit was then allowed to warm up and held at a certain temperature in the range from 14.0 to 18.0 K for solid Ar and from 13.5 to 15.5 K for solid N_2. For kinetic measurements, the temperature was kept constant to about ±0.1 K, and the uncertainty of the temperature measurement of the deposit was about 1 K. At each temperature, spectral changes were monitored by several sequentially measured IR spectra.

For the matrix experiments performed at La Plata University, gas mixtures of the samples in argon (1:1000) were prepared by standard manometric methods in a 1 L glass storage container. Those mixtures were deposited on a CsI window cooled at 16 K by means of a Displex closed-cycle refrigerator (SHI-APD Cryogenics, model DE-202) using the pulse deposition technique. IR spectra of each matrix sample were recorded at a resolution of 0.5 cm^{-1}, with 128 scans, and a CsI window at the cryostat using a Nexus Nicolet instrument equipped with MCTB and DTGS detectors for the ranges 4000−400 and 600−180 cm^{-1}, respectively. For photolysis experiments, the matrixes were exposed to broad-band UV−vis radiation ($200 \leq \lambda \leq 800$ nm) from a Spectra-Physics Hg−Xe arc lamp operating at 1000 W and using a quartz window at the cryostat and a water filter in

(48) Klapstein, D.; Nau, W. M. *Spectrochim. Acta* **1994**, *50A*, 307–316.
(49) Gombler, W.; Willner, H. *J. Phys. E: Sci. Instrum.* **1987**, *20*, 1286–1288.
(50) Schnöckel, H. G.; Willner, H. *Infrared Raman Spectrosc., Methods Appl.* **1994**, 297.

the output to absorb IR radiation and to minimize any heating effects.

d. UV Spectroscopy. UV−vis spectra of the gas phases of FC(O)SCN and FC(O)NCS were recorded using a glass cell equipped with quartz windows (10 cm optical path length) on a Lambda EZ210 UV−vis spectrometer (Perkin-Elmer). Measurements were carried out in the spectral region from 190 to 700 nm with a sampling interval of 1.0 nm, a scan speed of 200 nm min^{-1}, and a slit with of 2 nm.

e. NMR Spectroscopy. For ^{13}C NMR measurements, pure samples were flame-sealed in thin-walled 4-mm-o.d. tubes and placed in 5 mm NMR tubes. The NMR spectra were recorded on a Bruker Avance 400 spectrometer at 100.6 MHz and a Bruker AC-250 spectrometer. The samples were held at 243 K [FC(O)SCN] and 223 K [FC(O)NCS], and CD_3OD was used as an external lock and reference.

f. X-ray Diffraction at Low Temperature. An appropriate crystal of FC(O)SCN of ca. 0.5 mm diameter was obtained in a closed capillary by a miniature melting-zone procedure on an Oxford Diffraction Gemini E Ultra diffractometer, equipped with a 2K × 2K EOS CCD area detector, a four-circle κ goniometer, an Oxford Instruments cryojet, and sealed-tube Enhanced (Mo) and Enhanced Ultra (Cu) sources. For data collection, the Mo source emitting graphite-monochromatic Mo Kα radiation (λ = 0.710 73 Å) was used. The diffractometer was controlled by the *CrysAlis*^{Pro} graphical user interface software. Data collection for the sample was carried out at 150 K, in a 1024 × 1024 pixel mode using 2 × 2 pixel binning. Processing of the raw data, scaling of diffraction data, and application of an empirical absorption correction were completed by using the *CrysAlis*^{Pro} program. The solution of the structure was obtained by direct methods, which located the positions of all atoms. The final refinement was obtained by introducing anisotropic thermal parameters and the recommended weightings for all atoms. The maximum electron densities in the final difference Fourier map were located near the heavy atoms. All calculations were performed using the *SHELXTL*-plus package[51] for the structure determination and solution refinement and for the molecular graphics.

For FC(O)NCS, an appropriate crystal of ca. 0.5 mm diameter was obtained in a closed capillary on the diffractometer with a miniature melting-zone procedure. Crystallization took place during cooling of the sample from about 197 K to 183 K at a rate of 15 K h^{-1}. Data collection was performed at 150 K using a Bruker-AXS Kappa APEX-II diffractometer housed at a FR591 rotating anode equipped with Incoatec Helios graded multilayer optics, affording 22 705 measured reflections. The structure solution was carried out by direct methods and refinement by full-matrix least squares against F^2 to R1 = 0.037 [$I > 2\sigma(I)$], wR2 = 0.108, 109 parameters, absolute structure parameter = 0.00(8), S = 1.064, and residual electron density +0.5/−0.2 e $Å^{-3}$.

The full crystallographic data of FC(O)SCN and FC(O)NCS are available from the Cambridge Crystallographic Data Centre (CCDC 782990 and 783549, respectively). These data can be obtained free of charge via www.ccdc.cam.ac.uk/data_request/cif.

g. Theoretical Calculations. Quantum chemical calculations were performed using the program package *Gaussian 03*.[52] Scans of the potential energy surface, structure optimizations, and vibrational frequencies of various isomers of FC(O)SCN have been carried out by applying ab initio (MP2),[53] density functional theory (B3LYP),[54−57] and complete basis set CBS-QB3 methods.[58,59] Single-point energy calculations were performed at the CCSD(T)/6-311+G(d) level of approximation, using the MP2-optimized geometries. Natural population analysis and second-order donor−acceptor interaction energies were estimated at the MP2/6-311+G(d) level using the *NBO 3.1* program[60] linked to the *Gaussian 03* package. TSs for the unimolecular isomerization of FC(O)SCN to FC(O)NCS and for their internal *syn*−*anti* rotational interconversion were optimized by the Synchronous Transit-guided Quasi-Newton (STQN) method implemented by Schlegel et al.,[61] and barrier heights were calculated from the energies of the TSs and the stable structures, taking zero-point vibrational energies into account. A vibrational potential energy distribution (PED; see the Supporting Information, Table S5), indicating the contribution of each force constant to a certain fundamental, was performed for FC(O)SCN using the *ASYM40* program.[62] In the transformation of the ab initio Cartesian force field into an internal harmonic force field, the nonredundant internal coordinates as defined in Figure S7 and Table S6 in the Supporting Information are used. The simulated IR and Raman spectra were plotted using pure Lorentzian band shapes with a half-width at half-height of 10 and 4 cm^{-1}, respectively. The Raman activities (S_i) calculated with the *Gaussian 03* program were converted to relative Raman intensities (I_i) using eq 1 derived from the intensity theory of Raman scattering, where ν_0 is the exciting frequency (in cm^{-1}), ν_i is the vibrational wavenumber of each normal mode, and h, c, and k are constants.[63]

$$I_i = S_i \frac{(\nu_0 - \nu_i)^4}{\nu_i \left[1 - \exp\left(-\frac{hc\nu_i}{kT}\right)\right]} \quad (1)$$

Acknowledgment. The authors thank the Deutscher Akademischer Austauschdienst Germany (DAAD), Agencia Nacional de Promoción Científica y Técnica, Consejo Nacional de Investigaciones Científicas y Técnicas, Comisión de Investigaciones de la Provincia de Buenos Aires, Facultad de Ciencias Exactas, Universidad Nacional de La Plata (UNLP), and Departamento de Ciencias Básicas de la Universidad Nacional de Luján for financial support. L.A.R. gratefully acknowledges the DAAD, UNLP, and Bergische Universität Wuppertal. C.O. D.V. acknowledges the DAAD, which generously sponsors the DAAD Regional Program of Chemistry for Argentina supporting Latin−American students working on their Ph.D.'s in La Plata. H.B. and H.W. acknowledge support from the Deutsche Forschungsgemeinschaft and the Fonds der Chemischen Industrie.

Supporting Information Available: Absolute calculated energies of the *syn* conformers of FC(O)SCN and FC(O)NCS (Table S1), calculated natural and Mulliken atomic charges for FC(O)SCN and FC(O)NCS (Table S2), vibrational frequencies, intensities, and assignment of the bands obtained after photolysis of Ar-matrix-isolated FC(O)SCN (Table S3) and FC(O)NCS (Table S4), potential energy distribution (Table S5)

(51) Sheldrick, G. *Acta Crystallogr., Sect. A* **2008**, *64*, 112–122.
(52) Frisch, M. J.; et al. *Gaussian 03*; 2004.
(53) Møller, C.; Plesset, M. S. *Phys. Rev.* **1934**, *46*, 618.
(54) Becke, A. D. *J. Chem. Phys.* **1993**, *98*, 5648–5652.
(55) Lee, C.; Yang, W.; Parr, R. G. *Phys. Rev. B* **1988**, *37*, 785.
(56) Perdew, J. P.; Burke, K.; Ernzerhof, M. *Phys. Rev. Lett.* **1996**, *77*, 3865.
(57) Perdew, J. P.; Burke, K.; Ernzerhof, M. *Phys. Rev. Lett.* **1997**, *78*, 1396.
(58) Montgomery, J. J. A.; Frisch, M. J.; Ochterski, J. W.; Petersson, G. A. *J. Chem. Phys.* **1999**, *110*, 2822–2827.
(59) Montgomery, J. A.; Frisch, M. J.; Ochterski, J. W.; Petersson, G. A. *J. Chem. Phys.* **2000**, *112*, 6532–6542.
(60) Reed, A. E.; Curtiss, L. A.; Weinhold, F. *Chem. Rev.* **1988**, *88*, 899–926.
(61) Peng, C.; Ayala, P. Y.; Schlegel, H. B.; Frisch, M. J. *J. Comput. Chem.* **1996**, *17*, 49–56.
(62) Hedberg, L.; Mills, I. M. *J. Mol. Spectrosc.* **2000**, *203*, 82–95.
(63) Krishnakumar, V.; Keresztury, G.; Sundius, T.; Ramasamy, R. *J. Mol. Struct.* **2004**, *702*, 9–21.

and nonredundant coordinates (Table S6) for FC(O)SCN, IR (gas) spectra of liquid and solutions of FC(O)SCN (Figure S1), van't Hoff plot for the *syn*−*anti* interconversion of FC(O)SCN (Figure S2), time-dependent IR spectra of FC(O)NCS isolated in Ar at 15.1 K (Figure S3), ^{13}C NMR spectra for FC(O)SCN (Figure S4) and FC(O)NCS (Figure S6), UV−vis spectra of gaseous FC(O)SCN and FC(O)NCS (Figure S5), and internal coordinates for FC(O)SCN (Figure S7). This material is available free of charge via the Internet at http://pubs.acs.org.

Note Added after ASAP Publication. This paper was published on the Web on November 8, 2010, with a minor text error in the Abstract. The corrected version was reposted on November 29, 2010.